Published in final edited form as:

Front Microbiomes. 2022 ; 1: . doi:10.3389/frmbi.2022.994464.

Modulation of microbiome diversity and cytokine expression is influenced in a sex-dependent manner during aging

Sarah E. Webster[1], **Duncan Vos**[2], **Thomas L. Rothstein**[1], **Nichol E. Holodick**[1,*]

[1]Center for Immunobiology, Department of Investigative Medicine, Western Michigan University Homer Stryker M.D. School of Medicine, Kalamazoo, MI, USA

[2]Division of Epidemiology and Biostatics, Department of Biomedical Sciences, Western Michigan University Homer Stryker M.D. School of Medicine, Kalamazoo, MI, USA

Abstract

The microbiome and immune system have a unique interplay, which influences homeostasis within the organism. Both the microbiome and immune system play important roles in health and diseases of the aged including development of cancer, autoimmune disorders, and susceptibility to infection. Various groups have demonstrated divergent changes in the gut microbiota during aging, yet the compounding factor of biological sex within the context of aging remains incompletely understood, and little is known about the effect of housing location in the composition of gut microbiota in the context of both sex and age. To better understand the roles of sex, aging, and location in influencing the gut microbiome, we obtained normal healthy BALB/cByJ mice from a single source and aged male and female mice in two different geographical locations. The 16S rRNA was analyzed from fecal samples of these mice and cytokine levels were measured from serum.16S rRNA microbiome analysis indicated that both age and sex play a role in microbiome composition, whereas location plays a lesser role in the diversity present. Interestingly, microbiome changes occurred with alterations in serum expression of several

[*]**Correspondence:** Nichol Holodick, PhD, nichol.holodick@med.wmich.edu.

[6]Author Contributions

SW performed the experiments and analyzed and interpreted the data and was a major contributor to writing the manuscript. DV analyzed and interpreted the data. TR analyzed and interpreted the data and edited the manuscript. NH performed experiments, analyzed, and interpreted the data, and edited the manuscript. All authors read and approved the final manuscript.

[5]Conflict of Interest

The authors declare that the research was conducted in the absence of any commercial or financial relationships that could be construed as a potential conflict of interest.

[9]Contribution to the Field Statement

The gut microbiome is composed of hundreds of distinct bacterial species in the gut which play important roles in health and disease including development of cancer, autoimmune disorders, and mental health disease. Various groups have demonstrated divergent changes in the gut microbiota during aging, but studies have largely ignored the compounding factor of biological sex within the context of aging. Additonally, little is known about the effect of location in the composition of gut microbiota in laboratory mice. To better understand the role that sex, location, and aging play in the gut microbiome and its modulation through B lymphocytes, we obtained mice from a single source and aged male and female mice in two different geographical locations. A 16S rRNA microbiome analysis indicated that both age and sex play a role in microbiome composition; additionally, despite controls, location plays a role in the diversity present as well. Interestingly, these microbiome changes occurred with changes in serum expression of several different pro-inflammatory cytokines including IL-10 and IL-6, which were also both differentially regulated in context to sex and aging. As B-2 cells are known regulators of the gut microbiota, we explored the possible influence of B-1a cells in this system. We found that B-1a cells express IL-10 and IL-6 and therefore, may play a role in gut microbiome maintenance. Together, these data indicate that not only do sex and aging shape the diversity and composition of the gut microbiome, but B-1a cells may be influencing these changes along with location of housing, despite common animal sourcing, emphasizing the importance of these factors in the mechanism of development of the gut microbiome.

different cytokines including IL-10 and IL-6, which were also both differentially regulated in context to sex and aging. We found both IL-10 and IL-6 play a role in the constitutive expression of pSTAT-3 in CD5+ B-1 cells, which are known to regulate the microbiome. Additionally, significant correlations were found between cytokine expression and significantly abundant microbes. Based on these results, we conclude aging mice undergo sex-associated alterations in the gut microbiome and have a distinct cytokine profile. Further, there is significant interplay between B-1 cells and the microbiome which is influenced by aging in a sex-dependent manner. Together, these results illustrate the complex interrelationship among sex, aging, immunity, housing location, and the gut microbiome.

Keywords

microbiome; aging; sex; immune system; B-1 cells

1 Introduction

Both the microbiome and immune system change with advancing age. Age-related changes to the microbiome include decrease in microbial diversity, increase in pathobionts, and increased gut permeability (1,2). Changes in the composition of the microbiome are associated with the development of obesity and related metabolic disorders (3,4) maintenance of gut barrier integrity (5–7), intestinal pro- and anti-inflammatory balance (8,9), immune and cardio-metabolic health (10–12), and homeostasis of the gut-brain axis (13–15). To date, a large body of evidence has shown that older people maintain a compositionally distinct microbiota as compared with younger adults; these changes are associated with gradients in clinical frailty and inflammatory status (16). Alterations in the composition and function of the microbiome have been attributed to several factors including: senescence, changed lifestyle and dietary schedules, geographic location, lesser mobility, reduced intestinal function, altered gut morphology, recurrent infections, and weakened immune system strength (17–20). Age-related changes to the immune system include skewed hematopoiesis, reduced lymphopoiesis, impaired innate and adaptive immune responses, impaired memory response, increase in autoimmune disease, and chronic inflammation, all of which may be associated with microbiome dysbiosis (21–25). Since the microbiome regulates the host-immune system and the immune system regulates the microbiome, each can play inter-dependent and independent roles in such age-related changes contributing to various diseases of the aged (26–29).

Recent studies have demonstrated the important relationship between the microbiome and B cells in health and disease. The microbiota can influence early B cell development, B cell repertoire diversification, IgA production, IgE production, B cell metabolism, and activation and differentiation of B cells (30–35). Interestingly, commensal bacteria contain orthologues to a common systemic lupus erythematosus (SLE) autoantigen, and exposure to such bacterial orthologues can prime production of autoantibodies (36). Translocation of commensal bacteria has also been shown to lead to a SLE-like disease via an increase in IFN-gamma and subsequent autoantibody production (11). Gut dysbiosis and altered tryptophan metabolism have also been shown to contribute to autoimmunity in lupus-prone

mice (37), which carry the Sle2c1 locus leading to CD5+ B-1 cell expansion (38). Furthermore, commensal bacteria have been shown to activate monocytes leading to the conversion of CD5+ B-1 cells to 4–1BBL+ CD5+ B-1 cells, resulting in impaired insulin signaling (20). B-1 cells produce 80–90% of the natural IgM (39–41), which is present in serum in the absence of infection or intentional immunization and is required for many immune system functions (42–50). We recently demonstrated sex influences age-related changes in natural IgM and natural antibody producing CD5+ B-1 cells (51).

Importantly, the microbiome is an inherent factor shown to manifest sex-related differences; sex hormones have been shown to influence the microbiota composition and microbes can affect levels of sex hormones (2,52–55). Recently, it was found that disruption of the maternal-offspring transmission of microbes during important periods of development leads to long-term offspring health consequences with males more susceptible to these effects (56). Differences in the microbiota between sexes have also shown to play a role in response to vaccination (57). Additionally, it was shown in a model of type 1 diabetes that the gut microbiota alters the levels of sex hormones in mice and plays a role in regulation of autoimmune disease fate (55).

Given the changes of the gut microbiome demonstrated with age and sex separately, we sought to investigate linkages specifically between aging, sex, the microbiome, and the immune system at the same time in a controlled system. There are many confounding factors in human studies, including changes in diet, medications, housing status, and physical location that cannot be easily controlled, making it difficult to identify direct effects of sex- and age-related changes to the microbiome. In this study, we obtained healthy BALB/c-ByJ mice from a single source and aged male and female mice in two different locations. 16S rRNA microbiome analysis indicated age and sex play a large role in microbiota composition; additionally, the housing location of the mice influenced the composition of the gut microbiome. Mucosal IgA, IL-10, and IL-6 regulate the microbiome (11,58–61) and are produced by CD5+ B-1 cells (62–66). We have recently demonstrated aged male and female mice have significantly more serum IgA, whereas only aged female mice have increased numbers of CD5+ B-1 cells and serum IL-5 (51), which is required for maintenance and antibody secretion of CD5+ B-1 cells (67). Considering the differential changes we observed in the microbiome between young and aged male and female mice, we investigated whether there may be differences in serum cytokine levels in these mice. Interestingly, we observed changes in serum expression of several different cytokines including IFNγ, IL-1β, IL-10, and IL-6, which were altered in association with sex and age. We then asked whether IL-10 and/or IL-6 could affect CD5+ B-1 cell signaling. We found both IL-10 and IL-6 play a role in the constitutive expression of pSTAT-3 in CD5+ B-1 cells. Together these results demonstrate sex and age affect composition of the gut microbiome and serum cytokine expression, which can affect CD5+ B-1 cells.

2 Materials and Methods

2.1 Animals and Sample Collection

BALB/c-ByJ mice were purchased from The Jackson Laboratory (#001026; Bar Harbor, ME) at 6 weeks of age and were aged to either 3-months or 18–26-months of age

in one of two separate animal facilities: the Feinstein Institute for Medical Research (FIMR, Manhasset, NY) or Western Michigan University Homer Stryker M.D. School of Medicine (WMed, Kalamazoo, MI). All animals were housed in identical environments with 5 mice per cage with a 12-hour light/12-hour dark cycle and ad libitum to water and food. Specifically, mice housed at FIMR were fed LabDiet 5053 and the mice housed at WMed were fed LabDiet 5002, which are nearly identical certified rodent diets (Table S1); chemical, mineral, and vitamin composition are identical though 5002 contains both soybean oil and ground soybean hulls while 5053 only contains soybean oil. Additionally, the mice were housed in identical bedding (irradiated ¼ inch bed-o-cob) and cages (Allentown micro-isolator cages). Mice were cared for and handled in accordance with the Guide for the Care and Use of Laboratory Animals, National Institutes of Health, and institutional guidelines. All studies were approved by each institutional IACUC committee.

Fecal samples from young and aged mice were collected at the same time by clean catch and into a 1.5mL sterile collection tube before being placed on dry ice for shipment. After fecal collection, mice were euthanized by CO_2 overdose followed by bilateral pneumothorax. Serum was collected at the time of euthanasia from all mice; however, only serum samples from the mice at WMed were available for cytokine analysis. Samples from the FIMR were shipped on dry ice to Second Genome for analysis. Samples from WMed were shipped on dry ice to Veracet (an off shoot of Second Genome) for analysis.

2.2 16S rRNA Whole Microbiome Sequencing

2.2.1 Sample Isolation—Location/Batch one samples (FIMR) were run by Second Genome in which the nucleic acid isolation was performed with MoBio PowerMag Microbiome Kit (Carlsbad, CA) according to manufacturer's guidelines and optimized for high-throughput processing. Location/Batch two samples (WMed) were run by Veracet in which nucleic acid was isolated with the Qiagen MagAttract PowerMicrobiome DNA/RNA Kit according to manufacturer's guidelines and optimized for high-throughput processing. The MagAttract PowerMicrobiome DNA/RNA Kit was formerly sold by MoBio as PowerMag Microbiome Kit. All samples were quantified via the Quibit Quant-iT dsDNA High Sensitivity Kit (Invitrogen, Life Technologies, Grand Island, NY) to ensure samples met minimum concentration and mass of DNA.

2.2.2 Library Preparation—To enrich the sample for bacterial 16S V4 rDNA region, DNA was amplified using fusion primers designed against the surrounded conserved regions and were tailed with sequences to incorporate adapters and indexing barcodes (Illumina, San Diego, CA). The primer sequences (not including the barcode, linker, and pad sequences) used at Second Genome and Veracet are as follows: FWD:GTGYCAGCMGCCGCGGTAA; REV:GGACTACNVGGGTWTCTAAT. The PCR is the library prep step since the primers include barcodes, etc. Each sample was PCR amplified with two differently bar coded V4 fusion primers and PCR products were quantified by fluorometric method (Qubit or PicoGreen; Invitrogen, Life Technologies, Grand Island, NY). Samples that met post-PCR quantification minimum were pooled in an equimolar fashion and advanced for sequencing.

2.2.3 Profiling Method—A pool containing 16S V4 enriched, amplified, barcoded samples were loaded into a MiSeq reagent cartridge, and then onto the instrument along with the flow cell. After cluster formation on the MiSeq instrument, the amplicons were sequenced for 250 cycles with custom primers designed for paired-end sequencing.

2.3 16S rRNA Data Analysis Methods

2.3.1 Overview—The full data analysis pipeline for Veracet's Microbial Profiling Service incorporates several separate stages: pre-processing, summarization, normalization, alpha diversity metrics, beta diversity metrics, ordination/clustering, sample classification, and significance testing. Second Genome's analysis software package was used for statistical analysis.

2.3.2 OTU Selection—Sequenced paired-end reads were merged using USEARCH (68) and the resulting sequences were compared to a Veracet strain database using USEARCH. All sequences hitting a unique strain with an identity >99% were assigned a strain OTU. To ensure specificity of the strain hits, a difference of >0.25% between the identity of the best hit and the second-best hit was required. For each strain OTU, one of the match reads was selected as representative and all sequences were mapped by USEARCH against the strain OTU representatives to calculate strain abundances. The remaining non-strain sequences were quality filtered and dereplicated with USEARCH. Resulting unique sequences were then clustered at 97% by UPARSE (de novo OTU clustering;(69)) and a representative consensus sequence per de novo OTU was determined. The UPARSE clustering algorithm comprises a chimera filtering and discards likely chimeric OTUs. All non-strain sequences that passed the quality filtering were mapped to the representative consensus sequences to generate an abundance table for de novo OTUs. Representative OTU sequences were assigned taxonomic classification via mothur's Bayesian classifier, trained against the Greengenes reference database (70) of the 16S rRNA gene sequences clustered at 99%.

2.3.3 Summarization—After the taxa are identified for inclusion in the analysis, the values used for each taxa-sample intersection are populated with the abundance of reads assigned to each OTU in an "OTU table". A corresponding table of OTU Greengenes classification is generated as well.

2.3.4 Diversity Metrics—Alpha diversity is a measure of richness identified as the sum of unique OTUs found in each sample. Shannon diversity utilizes the richness of a sample along with the relative abundance of the present OTUs to calculate a diversity index. Signifiance between sample alpha-diversity metrics was determined using Chi-squared and Kruskal-Wallis.

Beta diversity was calculated by inter-comparing profiles in a pair-wise fashion to determine a dissimilarity score and store it in a distance dissimilarity matrix. The dissimilarity score produced by the distance function was used to compare samples with low dissimilarity scores and high dissimilarity scores, corresponding to similar samples and different samples, respectively. Abundance-weighted sample pair-wise differences were calculated using the Bray-Curtis dissimilarity as the ratio of the summed absolute differences in counts to the

sum of abundances in the two samples. The binary dissimilarity values were calculated with the Jaccard index to compare the number of mismatches (OTUs present in one but absent in the other) in two samples relative to the number of OTUs present in at least one of the samples.

2.3.5 Ordination, Clustering, and Classification Methods—Two-dimensional ordinations and hierarchical clustering maps of the samples in the form of dendrograms were created to graphically summarize the inter-sample relationships across age, sex, and location. Principal Coordinate Analysis (PCoA) is a method of two-dimensional ordination plotting that was used to help visualize complex relationships between samples. PCoA uses the sample-to-sample dissimilarity values to position the points relative to each other by maximizing the linear correlation between the dissimilarity values and the plot distances. Dendrograms were created using the Ward method of linkage for hierarchically clustering to evaluate hierarchical relationships between samples.

2.3.6 Whole Microbiome Significance Testing—Permutational Analysis of Variance (PERMANOVA) was utilized to determine dissimilarity measures. Veracet used a Conditional Monte Carlo (CMC) permutation test. The CMC test gives similar results to carrying out all possible permutations. In this randomization/Monte Carlo permutation test, the samples are randomly reassigned to the various sample categories, and the between-category differences are compared to the true between-category differences. The PERMANOVA utilized the sample-to-sample distance matrix directly, not a derived ordination or clustering outcome.

2.3.7 Taxon Significance Testing—Univariate differential abundance of OTUs was evaluated using a negative binomial noise model for the overdispersion and Poisson process intrinsic to this data, as implemented in the DESeq2 package and described for microbiome applications (71). This method accounts for both technical and biological variability between experimental conditions. Univariate differential abundance of OTUs is tested using a negative binomial noise model for the overdispersion and Poisson process intrinsic to this data, as implemented in the DESeq2 package and described for microbiome applications. It takes into account both technical and biological variability between experimental conditions. DESeq was run under default settings and q-values were calculated with the Benjamini-Hochberg procedure to correct p-values, controlling for false discovery rates. Features were only considered signifanct if their FDR-corrected P-value was less than or equal to 0.05 per Veracet.

2.4 Pro-Inflammatory and Cytokine Analysis

2.4.1 Serum Collection—Whole blood was collected from each individual BALB/c-ByJ naïve mouse at the time of the euthanasia at indicated age. Whole blood was allowed to clot at room temperature for 20 minutes before centrifugation and the supernatant (serum) was then collected. The serum was stored at −20°C until use.

2.4.2 V-PLEX Mouse Cytokine 19-plex Panel—Nineteen plasma cytokines (IFNγ, IL-1b, IL-2, IL-4, IL-5, IL-6, IL-9, KC/GRO, IL-10, IL-12p70, IL-15, IL-17A/F,

IL-27p28/IL-30, IL-33, IP-10, MCP-1, MIP-1a, MIP-2, TNF-a) were measured using chemiluminescence-based assays from Meso Scale Discovery (MSD; Gaithersburg, MD) using the V-PLEX 19 mouse cytokine 19-plex panel (MSD; catalog #K15255D-2). The detection ranges are IFNγ: 0.04–570 pg/mL IL-1β: 0.11–1030 pg/mL; IL-2: 0.22–1570 pg/mL; IL-4: 0.14–1060 pg/mL; IL-5: 0.07–590 pg/mL; IL-6: 0.61–3140 pg/mL; KC/GRO: 0.24–1230 pg/mL; IL-9: 3.84 – 2,600 pg/mL; IL-10: 0.95–2030 pg/mL; IL-12p70: 9.95–20 600 pg/mL; IL-15: 16.0 – 26,000 pg/mL; IL-17A/F: 0.231 – 1,620 pg/mL; IL-33: 0.364 – 1,950 pg/mL; IL-27p28/IL-30: 1.39 – 6,500 pg/mL; IP-10: 0.328 – 650 pg/mL; MCP-1: 0.672 – 325 pg/mL; MIP-1α: 0.081 – 390 pg/mL; MIP-2: 0.053 – 423 pg/mL; TNF-α: 0.13–403 pg/mL. All assays were performed in duplicate with at least n=5 animals for each age/sex group. Cytokine analysis was performed on serum samples obtained from the same WMed cohort of mice as the microbiome analysis. Serum IgA concentrations were obtained from WMed mice and performed in a previously published study (51), which were of the same cohort of mice used for microbiome analysis. Analyses were done using a QuickPlex SQ 120 instrument (MSD), DISCOVERY WORKBENCH 5.1 software (MSD), and GraphPad Prism. Results are shown for cytokine samples with a coefficient of variation (CV) <12 (IFNγ, IL-1β, IL-10, IL-6, IL-5, KC/GRO); therefore, results for cytokines with a high CV were not included. All samples were run at the same time.

2.5 Statistical and Correlation Analysis

Means and standard errors were calculated for the cytokine expression data using GraphPad Prism. To test significance, a two-way ANOVA was run with Tukey's multiple comparison test. Correlation analysis was performed to evaluate the relationship between strain abundance (using data from WMed & FMIR) and cytokine expression (using serum from WMed) for strains that significantly differed in relative abundance by age and sex. Non-linear Spearman Rank-order correlation was used to evaluate the strength of the correlation between strain abundance and cytokine expression with GraphPad Prism, calculating a Spearman correlation value for each strain and cytokine relationship (r value). The p-value associated with the Spearman Rank-order correlation was calculated within Prism (two-tailed). The resulting r values were then heat mapped against the logarithm base 10 of relative abundance (used to minimize the variation) using Morpheus matrix visualizion and analysis software (Morpheus, https://software.broadinstitute.org/morpheus). Scatter plots were provided for all significant correlations ($p<0.05$ and $\alpha<0.05$). Specific significance tests are listed on each figure legend.

2.6 Analysis of IL-6 and IL-10 on CD5+ B-1 cell signaling

2.6.1 Isolation of CD5+ B-1 cells—

Peritoneal lavage and spleen removals were performed on euthanized BALB/c-ByJ male mice. Spleens were homogenized using the frosted ends of microscope slides and then passed through a 70-um cell strainer. All samples were treated with RBC lysis buffer for 2 minutes (Lonza), subsequently diluted with HBSS with 2.5% FBS, and then centrifuged at 1200rpm for 10 minutes. The cells were resuspended in HBSS with 2.5% FBS, stained with immunofluorescent antibodies, and then sorted on an Influx cell sorter (BD Biosciences) with gating on live cells by forward side scatter. The following antibodies were obtained from BD Pharmingen: CD19 (clone ID3), B220/CD45 (clone RA3–6B2), and CD5 (clone 53–7.3).

2.6.2 pSTAT-3 detection in CD5+ B-1 cells after IL-6 and/or IL-10 neutralization—

Isolated CD5+ B-1 cells were treated with 10 μg/ml of anti-IL-6 (R&D Systems AF-406-NA) and/or anti-IL-10 (R&D Systems AB-417-NA) neutralizing antibody for 24 hours at 37°C. As a control for the effectiveness of each neutralizing antibody, B2 cells were stimulated with IL-6 and/or IL-10 (10 ng/ml) (R&D Systems) for 24 hours in the presence or absence of 10 ug/ml anti-IL-6 and/or anti- IL-10 (R&D Systems). In addition, we utilized a goat IgG antibody as a control for neutralization (R&D Systems). Afterwards, cells were pelleted, frozen, and lysed in NP-40 lysis buffer for western blot analysis of phosphorylated STAT3. Total protein was resolved on a 10% SDS-PAGE gel at 80 constant volts for about 2 hours. A protein standard was used to determine protein size (BioRad #1610374). A sandwich was prepared in between two sponges using two pieces of chromatography paper (Whatman #3030 917), the SDS PAGE gel, nitrocellulose pre-soaked in distilled water for 10 minutes, and then two more pieces of chromatography paper were stacked on top of the nitrocellulose, in that order. The separated proteins were then transferred to Hybond ECL nitrocellulose membrane (Amersham #RPN303D) at 100 volts for one hour using the Mini Trans-Blot Electrophoretic Transfer Cell (BioRad #170–3930). The membrane was then blocked with 5% non-fat dry milk in TBST (TBS, Tris Base, NaCl, 0.1% tween, pH 7.6) for one hour at room temperature with gentle rocking or rotating. The membrane was incubated with one of the antibodies, either Phospho-STAT3 (Ty705, Cell Signaling 9138) or STAT3 (Cell Signaling 9139) in 2% non-fat dry milk overnight at 4°C. Afterwards, the membrane was washed with Tris-buffered saline with 0.1% Tween-20 (TBST) once for 15 minutes and then three 5-minute washes. Next, the blot was probed with goat anti-mouse-IgG-HRP (Santa Cruz Biotechnology #sc-2005) for one hour at room temperature in 2% non-fat dry milk in TBST. Again, the membrane was washed with TBST once for 15 minutes and then three 5-minute washes. Detection was performed with enhanced chemiluminescence (Pierce #34080) and then developed with autoradiography film (Denville #E3012).

2.6.3 pSTAT-3 detection in CD5+ B-1 cells obtained from IL-6 or IL-10 knockout mice—

IL-10 knockout (B6.129P2-Il10^{tm1Cgn}/J, strain #002251) and IL- 6 knockout (B6.129S2-Il6^{tm1Kopf}/J, strain #002650) mice of 6–8 weeks age were obtained from The Jackson Laboratory (Bar Harbor, ME). Peritoneal lavage and spleen removals were performed on euthanized IL-10 and IL-6 knockout male mice. Spleens were homogenized using the frosted ends of microscope slides and then passed through a 70-um cell strainer. All samples were treated with RBC lysis buffer for 2 minutes (Lonza), subsequently diluted with HBSS with 2.5% FBS, and then centrifuged at 1200rpm for 10 minutes. The cells were resuspended in HBSS with 2.5% FBS, stained with immunofluorescent antibodies, and then sorted on an Influx cell sorter (BD Biosciences) with gating on live cells by forward side scatter. The following antibodies were obtained from BD Pharmingen: CD19 (clone ID3), B220/CD45 (clone RA3–6B2), and CD5 (clone 53–7.3). Isolated CD5+ B-1 cells were treated were pelleted, frozen, and lysed in NP-40 lysis buffer for western blot analysis of phosphorylated STAT3.

3 Results

3.1 Sample collection and sequencing of the 16S rRNA V4 region

A total of 40 healthy BALB/c-ByJ mice of two age groups; 10 females and 10 males between 2–4 months old (young group) and 10 females and 10 males between 18–26 months old (old group), were used for this study. The mice were housed and aged in two different locations (also referred to as batches) (Figure 1A). The two locations were The Feinstein Institute for Medical Research (FMIR) in Manhasset, NY (batch 1) and Western Michigan University Homer Stryker M.D. Medical School (WMed) in Kalamazoo, MI (batch 2). The bacterial community of the gut was analyzed from fecal collection from all animals (see Methods). The bacterial 16S rRNA gene V4 region (16S) was sequenced using Illumnia MiSeq to obtain a total of 12,231,644 total quality-filtered reads. For the 40 samples that were analyzed, the total number of reads per sample from each age and sex group was greater than 50,000.

Clustering of the high-quality 16S reads generated a total of 1,136 operational taxonomic units (OTUs) from all samples after removal of OTUs unclassified at the kingdom level; removal of spurious OTUs was completed by independent filtering with OTUs seen at least once within 5% of the data set being kept, reducing the number of OTUs to 842 (Supplemental Figure S1). Importantly, rarefaction curves for most samples approached saturation indicating that communities were sufficiently sampled to characterize the microbiome (Supplemental Fig S1). These data indicate that the sample size of the gut microbiome was sufficient to enumerate and cover the OTUs shared within the sequencing profiles. Within the sample populations, 100% of the kingdom taxa were identified, 99.93% of phylum taxa were identified, and 63.14% of the genus taxa were identified (Supplemental Figure S2).

3.2 No significant differences in alpha diversity of the microbiota between male and female mice of any age

First, the alpha diversity, or species richness, was analyzed based on the observed OTU number and the Shannon index (Figure 1B). These two metric analyses gave similar results, revealing the alpha diversity of the male microbiome was like that of the female microbiome; there were no significant differences in alpha diversity based on age. In females the average OTU richness was 439±31.5 (SD) while the average males were 426±62.1 (SD), with the Shannon diversity having an average of 3.97±0.475 (SD) and 4.17±0.24 (SD) respectively. This indicates that alpha diversity does not significantly differ by sex or age. We have summarized these findings in Supplemental Table 2. As there was no change in the alpha diversity driven by sex-dependent aging, we next examined changes to the beta diversity in these groups.

3.3 Differences in beta diversity in gut microbiome between age and sex groups

The overall structural similarly and variation (beta diversity between samples) between the microbiomes from the age and sex groups were then examined using the Bray-Curtis dissimilarity distance analysis with Principal Coordinates Analysis (PCoA). Assessment of these differences by the Permutational Multivariate Analysis of Variance (PERMANOVA)

showed that age group, sex, and location (batch) all significantly contributed to the beta diversity of the samples (Figure 2A). Interestingly, Bray-Curtis weighted ordination showed that the microbiome samples tended to cluster according to age and to a lesser degree by sex (Figure 2B), while unweighted ordination clustered according to location (batch) (Supplemental Figure S2). As samples separated by location on unweighted ordination, this indicates that there are substantial differences in the number and presence of OTUs detected between samples. However, this difference was not strongly observed in the weighted ordination which considers relative abundance of OTUs as well as presence/absence.

Hierarchical clustering demonstrates these data partially separated by age, sex, and location (Figure 2C). These data confirm previous reports of age-related alterations of the gut microbiome (17,19,21–23) and demonstrate for the first time that sex-related alterations also play a role in the relative abundance and community species membership of the gut microbiome in the context of aging.

3.4 Taxonomic profiles of gut microbiomes differ between the age and sex groups and are influenced by location

Since the beta diversity analysis indicated clustering primarily between age and sex, we examined specific comparisons between age and sex groups. First, a comparison between all old and young mice was performed (Figure 3A). The differential expression of the microbial diversity was apparent between these two groups. The comparison of the proportional abundance of all aged mice versus all young mice indicated that the *TM7* phylum was significantly ($p<0.001$; Kruskal-Wallis) more abundant in aged mice (0.149±0.082%) than young mice (0.000482±0.00026%), while *Verrucomicrobia* (4.76±1.0644% vs 0.447±0.100%; $p<0.001$) and *Tenericutes* (4.15±0.928% vs 1.04±0.2326%; $p<0.001$) were more abundant in young mice compared to aged mice, respectively (Figure 3A). At the family level, significant differences were observed in *Rikenellaceae,* in which the aged population had higher abundance (4.68±1.05% vs 2.17±0.49%; $p<0.05$) and *Clostridiales* family 91otu457, in which the young had higher abundance (1.91±0.43% vs 3.44±0.77%; $p<0.01$) (Figure 3B). The first two ordination axes using the PCoA for the weighted ordination across age and sex accounted for 27.9% of sample variation (Figure 3C). Further analysis between the OTUs in the old and young populations showed that there were 170 significantly different features detected out of 842 tested, with a $\log_2$-fold change greater than 1 and a Benjamini-Hochberg corrected $p<0.05$ (Figure 3D). In old mice, the top enriched features were from *Candidatus*, 94otu17563, 94otu13307, and 94otu10153 genera while young mice were enriched in *Dorea*, 94otu11038, and 94otu20054 genera. Specifically, at the strain level, *Streptococcus* sp. and *Lactobacillus intestinalis* were enriched in the old group ($p=4.37e^{-6}$ and $p=1.06e^{-5}$) while *Akkermansia muciniphila* ($p=3.60e^{-4}$) was enriched in the young population (Figure 3E).

To further explore these age-related changes in microbiota, we compared aged males to young males (Figure 4A). *Verrucomicrobia* and *Tenericutes* were significantly more abundant in young male mice than old male mice (Figure 4A). Specifically, young male mice had significantly more *Verrucomicrobaceae* and *Ruminococcaceae* than old male mice, while old male mice were enriched with an unclassified family. The first two ordination

axes using the PCoA for the weighted ordination across age accounted for 35.5% of sample variation (Figure 4B). Additionally, hierarchical clustering partially separated the males by age as well (Supplemental Figure 3A). Between young and old male mice, there were 99 significantly different features detected out of 783 tested, with 56 OTUs enriched in old mice while 43 OTUs were enriched in young mice (Figure 4C). Specifically, two significant OTUs were identified at the strain level; *Akkermansia muciniphila* was enriched in the young male population ($p=0.019$) while *Clostridium disporicum* was enriched in the old male population ($p=0.0035$). Comparatively, aged female mice were then profiled against young female mice (Figure 4D). By phyla, old female mice had a significantly higher abundance of *TM7* while young female mice had a higher abundance of *Tenericutes* (Figure 4D). Young female mice specifically had a higher abundance of an unclassified family. The first two ordination axes using the PCoA for the weighted ordination across age accounted for 43.3% of sample variation (Figure 4E). Hierarchical clustering analysis additionally showed sample separation by age between old and young females (Supplemental Figure 3B). Significantly different abundance features were found between young and old females; specifically, there were 157 significantly different features detected out of 800 tested, 97 of these being from old female mice and 60 enriched in young female mice (Figure 4F). At the strain level, four significant OTUs were identified: *Streptococcus* sp., *Lactobacillus intestinalis*, and *Lactobacillus reuteri* were enriched in old female mice while *Akkermansia muciniphila* was enriched in young female mice.

Next, we compared the microbiomes between males and females in the same age groups to better understand the specific differences due to sex. First, we compared all aged male mice with aged female mice in which we saw significant changes in beta diversity; female mice had significantly higher relative abundance of both *Proteobactera* and *TM7* phylum, though at the family level, significant enrichment was seen in aged males in both an unclassified family was well as *Ruminococcaceae* (Figure 5A). There was clear separation based on sex when weighted ordination was performed between aged males and females (Figure 5B). Samples also partially separated by sex based on hierarchical clustering (Supplemental Figure 4A). There were 97 significantly different OTUs with 55 enriched in aged female mice and 42 enriched in aged male mice (Figure 5C). Of these, two strain-level OTUs were identified; both *Clostridium saccharogumia* and *Lactobacillus intestinalis* were enriched in aged females compared to aged males. We then compared the microbiota of young male mice to that of young female mice. Specifically, at the phylum level, *Cyanobacteria* was significantly more abundant in young male mice (Figure 5D) than young female mice. At the family level, *Ruminococcaceae* were increased in young male mice while an unclassified family was increased in young female mice (Figure 5D). Despite these changes, weighted ordination using abundance of OTUs showed no separation by sex, but rather partial separation based on location (Figure 5E). However, hierarchical clustering by Ward's method and with Bray-Curtis distance, partial separation by sex between young male and female mice was seen (Supplemental Figure 4B). Interestingly, 41 OTUs were enriched in young female mice while 54 were enriched in young male mice (Figure 5F); specific changes in strains were seen in an enrichment of *Lactobacillus gasseri* in young females while young males had an enrichment in *Ruminococcaceae bacterium* D16. Together, these data demonstrate changes in the gut microbiota are associated not only with aging but also

with sex and somewhat by location. We then asked how the immune system may be involved in the regulation of these changes.

3.5 Serum cytokine levels are changed in relation to sex in aging mice

Cytokines play a key role in coordinating immune responses including inflammation and pathogen defense (72–75). Given the many examples of microbiota modulating immune responses, we investigated the relationship of cytokine responses between these young and old male and female mice. We analyzed several circulating cytokines (IFNγ, IL-10, IL-1β, IL-6, and KC/GRO) from serum collected from young and aged, male, and female mice at the Michigan (WMed) location. We found that cytokine levels exhibited a wide range in each group; average expression levels of IFNγ, IL-10, IL-1β, and IL-6 were found to be significantly differentially expressed between age- and sex-groups while KC/GRO was not (Figure 6).

First, we looked at pro-inflammatory cytokines. IFNγ plays an essential role in promotion of the adaptive immune response and immunoregulatory functions (76). We found that serum levels of IFNγ changes with both sex and age. Interestingly, IFNγ increases significantly with age in females (0.87pg/mL to 2.6 pg/mL; $p<0.001$). Overall, the level of IFNγ is higher in females compared to males and increases in aged females as compared to young females (Figure 6A). Next, we examined KC/GRO, which signals through CXCR1 or CXCR2 receptors; in general, KC/GRO proteins chemoattract and activate various monocytes including neutrophils and basophils functioning in inflammation and wound healing (77). Changes in expression were not significantly different between any age-group nor based on sex (Figure 6B). We also examined IL-1β serum levels; IL-1β is considered a trigger for the inflammatory cascade. It functions in a proinflammatory manner causing fever, liver acute-phase response, and even cognitive decline (78,79). Here, we found serum IL-1β levels are highest in young males (4.35pg/mL) while the levels are significantly lower in young females (3.03pg/mL, $p=0.0047$; Figure 6C). Interestingly, as mice age, IL-1β levels decrease in both males and females to 3.25pg/mL and 2.23pg/mL, respectively, but this decrease only reaches significance in males (aged males vs young males; $p=0.0043$; aged females vs young females; $p>0.05$). The expression patterns of IL-1β are the most diverse of the cytokines we examined inasmuch as young males express the highest amounts while aged females express the lowest amounts of IL-1β. In addition, we examined expression of serum IL-6. IL-6 is a multi-functional cytokine, and its increase in circulation with age is considered an important marker of acute inflammatory stress (78). In agreement with previous literature, we found that IL-6 increases with age, but is more significantly increased in females compared to males, a change from 4.686pg/mL to 12.26pg/mL in males ($p=0.0043$) whereas females increased from 4.47pg/mL to 24.34pg/mL ($p=0.0030$; Figure 6D). Lastly, we examined the anti-inflammatory cytokine, IL-10. One of the ways IL-10 functions is to inhibit TNFα/IL-1 production (80). Expression levels of IL-10 in aged females were extremely variable, with levels as high as 87.71pg/mL (Figure 6E). On average, young males, young females, and aged males express levels between 6.2pg/mL (young female) to 7.72pg/mL (young male) while the average of aged females is 33.92pg/mL ($p<0.05$ vs old males; $p<0.01$ vs young females). This large increase unique to aged females is interesting as IL-10 has been shown recently to prevent age-

associated inflammation (81) and historically has been shown to prevent other age-induced dysfunctions (82).

Taken together, there are significant changes in serum cytokine expression associated with aging in a sex-specific manner; particularly, we found that IFNγ and IL-10 were increased in aged females exclusively, while IL-6 was increased in both aged male and female mice. We were interested to then determine if these age- and sex-specific changes in cytokine expression were associated with the changes in microbial diversity previously observed.

3.6 Highly abundant gut microbial species show direct association with serum cytokine levels in an age- and sex-specific manner

To determine any significant relationships between serum cytokine expression and microbial composition, we performed pairwise correlation tests between microbial taxonomic composition at the strain level that were significantly changed and each cytokine in relation to both age and sex (Spearman correlation with $\alpha < 0.05$ an a two-tailed $p<0.05$; Figure 7A). A total of 19 significant interactions were identified. When young males were analyzed alone, there were no significant correlations with any bacterial strain and cytokine expression. Young females however, had positives correlations between IL-10 and *L. gasseri* (r=0.6753; $p<0.05$), IL-1β and *L. reuteri* (r=0.792; $p<0.05$), and IL-6 was negatively correlated with *R. bacterium* (r= −0.8182; $p<0.01$). These correlations are shown in Figure 7B. Old males had only a negative correlation with *A. municipalis* and KC/GRO (r= −1; $p<0.01$; Figure 7B) while old females had several significant correlations; *C. saccharogumia*, *L. intestinalis*, and *C. disporcium* were all positively correlated with KC/GRO (Figure 7B). In addition, serum IgA was negatively correlated with *A. muciniphila* in aged females (r= −0.6727; $p<0.05$).

We then examined correlations between our larger variables singularly; that of sex and that of age. In the young (Supplemental Figure S5), the sole significant correlation was a positive correlation between *A. municipalis* and IL-6. However, in the old, several strains were significantly correlated with several cytokines. *Streptococcus* sp. ERD01G was negatively correlated with IFNγ (r = −0.6203; $p<0.05$) and positively correlated with IL-1β (r = 0.7837; $p<0.01$). *C. saccharogumia* was positively correlated with KC/GRO (r = 0.5385; $p<0.05$) as was *C. disporicum* (r = 0.549; $p<0.05$). When sex was examined alone in all males (Supplemental Figure S6), IFNγ was positively correlated with *R. bacterium* (r=0.7636; $p<0.01$) and IL-6 was negatively correlated with *A. municipalis* (r=−0.6742; $p<0.05$) in all males. In all females, a correlation was seen in *L. reuteri* negatively with IL-10 (r= −0.6149; $p<0.01$) but positively with IL-1β (r = 0.6628; $p<0.01$). Interestingly, IL-6 was negatively correlated with *Streptococcus* spp. (r= −0.6223; $p<0.05$) and *C. disporcium* was positively correlated with KC/GRO (r= 0.5976; $p<0.01$; Supplemental Figure S6).

Together, these data demonstrate that there are important links to the repertoire of serum cytokines and the composition of the microbiome. Importantly, these changes are most noted when looking specifically at the role of sex (male vs female) or age (old vs young). Specifically, we were most interested in IL-10 and IL-6 as they were differentially expressed (Figure 6) and displayed significant correlations with bacterial species abundance (Figure 7

+ Supplemental Figures S5 and S6). As B-1 cells are known to produce IL-6, IL-10, and IgA (62–66), which have all been shown to regulate the microbiome, we further explored the role of IL-10 and IL-6 in the signaling of B-1 cells.

3.7 IL-10 and IL-6 provide the signal to activate STAT-3 in peritoneal CD5+ B-1 cells

B lymphocytes are involved in the regulation of the gut microbiome through production of IgA (83). CD5+ B-1 cells have been shown to produce approximately half of the gut IgA (66,84). Interestingly, naïve CD5+ B-1 cells exhibit constitutive activation of STAT3, which is activated downstream of either IL-10 or IL-6 binding their respective receptors. Considering our results demonstrating differences in serum levels of both IL-10 and IL-6, we asked whether these cytokines could contribute to the constitutive activation of STAT3 in CD5+ B-1 cells. Sort purified CD5+ B-1 cells were treated with anti-IL-6 and/or anti-IL-10 neutralizing antibody for 24 hours (Figure 8). Afterwards, cells were pelleted, frozen and lysed for western blot analysis of phosphorylated STAT3 (pSTAT3). As a control for the effectiveness of each neutralizing antibody, B2 cells were stimulated with IL-6 and/or IL-10 for 24 hours in the presence or absence of anti-IL-6 and/or anti- IL-10. Figure 8A shows B2 cells cultured for 24 hours with IL-6 and IL-10 have phosphorylated STAT3, which is blocked when B2 cells are co-cultured with IL-10, IL-6, anti-IL-10 and anti-IL6. These results demonstrate the effectiveness of the neutralizing IL-6 antibody. Relative pSTAT3 expression from at least four independent experiments including a goat IgG control antibody is presented in Figure 8B. Relative pSTAT3 expression was calculated by normalization to total STAT3 by densitometry analysis of scanned gels. Statistical analysis was performed comparing anti-IL-6, anti-IL-10, or anti-IL-6 plus anti-IL-10 to the goat IgG control, which demonstrated all had significantly lowered pSTAT3 protein levels as compared to the IgG control antibody. The pSTAT3 protein levels in the presence of both anti-IL-10 and anti-IL-6 antibodies were not lowered to the same extent as anti-IL-6 alone. The reason for such a discrepancy is unknown. It has been previously shown LIF is involved in the constitutive STAT3 activation observed in CD25 positive CD5+ B-1 cells (85), which could account for the differences seen. To confirm the IL-6/IL-10 neutralization studies, we examined STAT3 activation in CD5+ B-1 cells obtained from IL-6 and IL-10 knockout mice. Figure 8C shows a representative western blot of phospho-STAT3 in CD5+ B-1 cells from IL-6 and IL-10 knockout mice. We found a decrease in phosphorylated STAT3 in both IL-6 and IL-10 knockouts (Figure 8D). Together, these results show neutralization or complete lack of IL-6 or IL-10 significantly reduces constitutive pSTAT3 in CD5+ B-1 cells. These results suggest higher serum levels of IL-6 and IL-10 may affect the B-1 CD5+ B-1 cell population, which plays a role in regulation of the microbiome.

4 Discussion

There is tremendous interplay between the immune system and the microbes within the body, which makes differentiating the two difficult as both are interdependent for homeostasis. Therefore, the microbiome as an entity could be thought to include both immune components as well as microbes. Studies have shown the influence of intrinsic (age, sex, genetics) and extrinsic (environment, therapeutics) factors upon the immune system and the microbiome in healthy and diseased states; however, these studies have

examined such factors independently. Herein, we examine in the same study, how sex and geographical location influence the complete microbiome in context of healthy aging. Our results demonstrate significant differences in the aging-microbiome in a sex-specific manner. Aging accounted for the most change in the microbiome when age, sex, and location were explored, though sex and location played a significant role as well. Healthy aging accounted for large changes in commensal bacteria diversity. Consistent with previous literature, both young and aging mice maintained a high percentage of *Firmicutes* and *Bacteroidetes.* However, aging mice lost abundance of *Verrucomicrobia* and *Tenericutes* as compared to young mice. Interestingly, abundance of TM7 was increased in healthy aged mice. The loss of TM7 is noteworthy as a more penetrable mucus layer is associated with high prevalence of this bacterial phylum (86); additionally, this phylum is also proposed to play a role in intestinal inflammation (87). This data would suggest that healthy aging predisposes the gut to inflammation and a more permeable mucus layer. Supporting this further, we found *Akkermansia muciniphila* was enriched in both young males and young females as compared to aged mice. The loss of *A. muciniphila* with age is consistent with previously published literature (9,88,89); however, this is the first study to our knowledge that determined that age-related loss of *A. muciniphila* is not influenced by other variables such as sex or location. Furthermore, aged mice also had increased abundance of *Lactobacillus intestinalis*, which has been previously associated with metabolic syndrome development (90,91) but, to our knowledge, not previously associated with healthy aging. These data highlight the important changes to the microbiome composition associated with healthy aging in the context of sex.

An interesting finding of this work was the hierarchy of influence between sex, aging and environment. From this study, we found that aging is the most impactful variable on gut microbial composition, followed by sex and then by environment. For example, previous literature found that *L. intestinalis* was increased in very young female mice as compared to very young males (2); however, in the work presented herein, we found that aged females had increased expression of *L. intestinalis* as compared to both aged males but also young females. As such, in our study we were able to specifically compare the changes in diversity associated with sex-specific aging. At the strain level, young males had higher abundance of *A. muciniphila* while aged males were enriched for *Clostridium disporicum*. Similarly, young females were enriched for *A. muciniphila*, while aged females were enriched for *Streptococcus* sp. ERD01G, *Lactobacillus intestinalis*, and *Lactobacillus reuteri*. When males and females were compared in each age group, we found that in aged mice, *Clostridium saccharogumia and L. intestinalis* were enriched in females. In young mice, *Lactobacillus gasseri* was enriched in young females while *Ruminococcacae bacterium* was enriched in young males. The role of biological sex in driving the composition of the microbiome has been largely ignored. It has been previously described that genetic background was a stronger determinant of shaping the microbiome composition than sex differences (92); in this study, we found similarly that sex wasn't the primary driver of microbiome diversity but importantly here, we describe those changes specifically due to sex as they are significant. As we described here, certain changes to the microbiome composition can be attributed to sex-differences primarily, an important

factor that previously has been given little attention. Our results clearly demonstrate that sex influences the composition of the aging gut microbiome in the context of age.

Importantly, the environment does play a role in microbiome composition, despite controls used in the laboratory setting. Previous work has demonstrated that the animal facility setting influences the composition of the microbiome due to various factors; however, this study examined young male mice exclusively (93). Here, we examined whether the animal facility influences the composition in relation to aging and biological sex. In the experiments presented here, all mice were housed in comparable AAALAC-approved facilities with identical light-dark cycles, cages, bedding, frequency of cage changes, and comparable food. When all samples were compared, through unweighted ordination and hierarchal clustering, location became a basis for separation. Further, when we examined only the young population by PCoA weighted ordination, the samples separated primarily by location and partially by sex. Further, PERMAOVA microbiome covariate significance identified location as a variable that significantly contributed to the beta diversity of samples. These data raise the unexpected possibility of mouse microbiome differences reflecting fomites from human handlers. As the microbiome can influence immune parameters, this adds another dimension to the issue with respect to reproducibility and universality of experimental results from any given laboratory. Previously, it has been recognized that different genetic strains may be manifesting different immune parameters and responses (94); herein we show location of experimentation should be considered in addition to age and sex in terms of particulars that may influence findings in mice. Such differences in bacterial strains present in the mouse microbiota has been previously appreciated in mice obtained from different vendors, which affected the frequency of Th17 cells (95).

The microbiome plays critical roles in the development of the immune system while the immune system maintains key features of host-microbe homeostasis (96) yet, the effects of sex during the aging process in these relationships are not well understood. Herein, we found serum cytokine levels to be differentially expressed between aged females and males. Aging has been shown to significantly change the landscape of cytokine production; some biomarkers of aging include increased levels in IL-6, which leads to bone and muscle loss, fever, activation of hepatic acute phase response, and decline in haemoglobin levels (78). In addition, the anti-inflammatory cytokine IL-10 produced by both innate and lymphoid cells, has been reported to increase in elderly people (97). Herein, we examine these and other cytokines; we found that aged females have elevated levels of serum IL-6, IL-10, and IFNγ as compared to young females whereas aged males have elevated levels of IL-6 as compared to young males. Figure 9 summarizes these findings. Since cytokines have been shown to play a role in the microbiome (98–101), the changes in cytokine levels we observed with age and sex could impact microbiome homeostasis.

Examining the interactions between the serum cytokine levels and abundance of specific strains, we found that there were several significant correlations. The increase in IL-6 during the aging process is interesting in context to the microbiome. Previous literature has shown that IL-6 is required for a robust mucosal barrier and effective communication between gut epithelial cells and immune cells (reviewed in (99)). Here, we found that IL-6 is positively correlated with *A. muciniphila* in young mice. IL-10 has previously been shown to be

produced by B cells in the gut to maintain specific microbial components (102). Herein, we found IL-10 to be positively correlated with *L. gasseri* in young females. Based on the analysis done in this study, there are significant correlations between serum cytokine profile and maintenance of abundance of commensal bacteria. Sex hormones have also been shown to modulate the expression of cytokines, though there are large gaps in our understanding of the specifics of this modulation. For example, testosterone, which declines in aging males, suppresses IL-6 and IL-1β in humans (103). Additionally, it has been shown in both mice and humans, that IL-2 and IFNγ are produced by lymphocytes stimulated with dehydroepiandrosterone sulphate (DHEA-S) (104,105) further indicating sex hormones may influence the active state of the immune system. What is unclear is whether cytokine production is due to the direct activation of immune cells by hormones, or rather by an indirect/secondary effect. Commensal bacteria have also been shown to provide an alternate source of hormones (reviewed in (106)). These previous studies and the results herein demonstrate the integral connections between microbiota, immune mediators, endocrine mediators, and age.

It has been well established that diet impacts the composition and function of the microbiome (reviewed in (107)). Recently, more attention has been drawn to the role of diet in the reproducibility of microbiome work in the laboratory (108). Slight changes were seen in the microbiome with varying diets however, the specific elements within the diets causing the changes in microbiota composition could not be elucidated. Here, we examined the role of two different animal housing locations in context to aging and sex in microbiome composition. We found location does play a role in microbiome diversity but that it is tertiary to that of age and sex. However, our experimental paradigm while nearly identical in housing varies in a few ways: 1) the human handlers for the animal rooms, 2) the composition of the deionized water, and 3) the small difference in diet. As compared to FMIR, mice at WMed were fed diets that consisted of additionally ground soybean hulls and casein (Supplemental Table S1). Interestingly, work has shown that both soy and bovine products can influence the gut microbiome when fed a high-fat diet (109). However, it is unclear if these specific dietary changes can influence the gut microbiome in context to aging in both males and females. Additionally, as the specific chemical content of diet differs lot to lot, further work exploring these variables is warranted.

CD5+ B-1 cells can secrete both IL-6 and IL-10 (62,63,110). Here, we demonstrate that IL-6 and IL-10 are, in part, responsible for the constitutive activation of STAT3 seen in CD5+ B-1 cells, which has also been shown to be downstream of LIF signalling (85). CD5+ B-1 cells play a role in regulation of the microbiome as they produce a significant proportion of mucosal IgA (66,111–113). It is currently unknown how altered cytokine levels and/or microbial diversity may affect mucosal CD5+ B-1 cells and their role in microbiome homeostasis; however, we recently demonstrated peritoneal CD5+ B-1 cells display sex-specific differential expression of *Irgm1* in the aged (51). Interestingly, the IFNγ-modulating gene *Irgm1* has been identified as regulating the abundance of *A. muciniphila,* where higher levels of *Irgm1* expression are shown to downregulate the activity and abundance of these bacteria (88,114). Recent work has demonstrated that *A. muciniphila constitutes* 3–5% of the healthy adult human microbiome, but the levels vary according to many factors including aging; reduced abundance of *A. muciniphila* is one of the first hallmarks of a dysregulated

microbiome (20,88,89,115). Our results demonstrate that the aging process results in the loss of *A. muciniphila* and this is not sex dependent. Interestingly, IFNγ can increase expression of *Irgm1* in a negative feedback loop (116) and loss of *Irgm1* has been shown to induce increased cytokine production and increased intestinal inflammation (117,118). We previously demonstrated CD5+ B-1 cells obtained from aged females show no change in *Irgm1* expression (51). Taken together, our data suggest that the loss of *A. muciniphila* we observe in aged mice is not due to *Irgm1*-specific downregulation by CD5+ B-1 cells. Yet, we observe increased IL-6 expression in both male and female mice, which could lead to an over production of IgA (119) and in turn, possibly negatively regulate the percent abundance of beneficial bacteria, such as *A. munícinipila*. Interestingly, we have observed a significant increase in serum IgA levels in aged males and females (51) and importantly, these increased levels of IgA in females does significantly correlate with the loss of *A. muciniphila* (Figure 7). However, it remains unknown if B-1 B cells are influencing the composition of the microbiome in this sex-specific manner or if the microbiome is regulating these developmental changes associated with aging B-1 cells. Further work is required to better understand this important relationship.

Our results demonstrate that the composition of the microbiome is associated with changes in age, sex, and housing environment of mice. Furthermore, we show aged mice had higher relative abundance of TM7 species and lower relative abundance of *Verrucomicrobia* and *Tenericutes* than the young mice. Further, regardless of sex, aged mice had lower relative abundance of *A. municiphila*, an important microbe known to be associated with gut health (89). In support of these findings, a recent publication in C57BL/6J males across lifespan was also shown to have an age-associated loss of *A. municiphila* (120). Interestingly, many differences in the microbiome were also associated sex, with more pronounced sex-specific differences in the aged population. Interestingly, when sex-specific differences are examined in the young population, they are present but influenced more by the location in which the animals were raised. We conclude that aging mice undergo sex-associated alterations in the gut microbiome with a distinct serum cytokine profile.

Immunological profiles are distinct in males and females; increased expression of IL-6 was seen in aging mice while increased expression of IL-10 was seen in aging female mice exclusively. We further demonstrated that IL-10 and IL-6 activate STAT-3 in CD5+ B-1 cells, which play a role in microbiome maintenance through IgA production (66,111–113). Importantly, differentially abundant microbes in aged animals show direct associations with serum cytokine levels including IL-1β, IL-10, IL-6, IFNγ, and KC/GRO as seen with correlation analysis. In conclusion, both age and sex play a significant role in the relationship between the immune system and the microbiome.

Supplementary Material

Refer to Web version on PubMed Central for supplementary material.

Acknowledgments

A sincere thank you to Mireya del Carmen Diaz Insua and Michael Clemente for thoughtful and helpful discussions on data analysis and manuscript preparation. We also acknowledge the outstanding technical support from the Flow Cytometry and Imaging Core at WMU Homer Stryker M.D. School of Medicine.

8 Funding

Funding was provided by the National Institute of Allergy and Infectious Diseases of the NIH under R01AI154539 (NH) and NIH AI029690 (TR). The content is solely the responsibility of the authors and does not necessarily represent the official views of the National Institutes of Health.

10 Data Availability Statement

The dataset generated and/or analyzed during the current study are available in NCBI Sequence Read Archive (SRA) repository, accension number PRJN810444; https://www.ncbi.nlm.nih.gov/sra/PRJNA810444

11 References

1. Falony G, Joossens M, Vieira-Silva S, Wang J, Darzi Y, Faust K, Kurilshikov A, Bonder MJ, Valles-Colomer M, Vandeputte D, et al. Population-level analysis of gut microbiome variation. Science (80-) (2016) 352:560–564. doi:10.1126/science.aad3503
2. Elderman M, Hugenholtz F, Belzer C, Boekschoten M, van Beek A, de Haan B, Savelkoul H, de Vos P, Faas M. Sex and strain dependent differences in mucosal immunology and microbiota composition in mice. Biol Sex Differ (2018) 9:26. doi:10.1186/s13293-018-0186-6 [PubMed: 29914546]
3. Tilg H, Kaser A. Gut microbiome, obesity, and metabolic dysfunction. J Clin Invest (2011) 121:2126–2132. doi:10.1172/JCI58109 [PubMed: 21633181]
4. Ley RE. Obesity and the human microbiome. Curr Opin Gastroenterol (2010) 26:5–11. doi:10.1097/MOG.0b013e328333d751 [PubMed: 19901833]
5. Gwak MG, Chang SY. Gut-brain connection: Microbiome, gut barrier, and environmental sensors. Immune Netw (2021) 21:1–18. doi:10.4110/in.2021.21.e20
6. Turner JR. Intestinal mucosal barrier function in health and disease. Nat Rev Immunol (2009) 9:799–809. doi:10.1038/nri2653 [PubMed: 19855405]
7. Jandhyala SM, Talukdar R, Subramanyam C, Vuyyuru H, Sasikala M, Reddy DN. Role of the normal gut microbiota. World J Gastroenterol (2015) 21:8836–8847. doi:10.3748/wjg.v21.i29.8787 [PubMed: 26269673]
8. Bolte LA, Vich Vila A, Imhann F, Collij V, Gacesa R, Peters V, Wijmenga C, Kurilshikov A, Campmans-Kuijpers MJE, Fu J, et al. Long-term dietary patterns are associated with pro-inflammatory and anti-inflammatory features of the gut microbiome. Gut (2021) 70:1287–1298. doi:10.1136/gutjnl-2020-322670 [PubMed: 33811041]
9. Desai MS, Seekatz AM, Koropatkin NM, Kamada N, Hickey CA, Wolter M, Pudlo NA, Kitamoto S, Terrapon N, Muller A, et al. A Dietary Fiber-Deprived Gut Microbiota Degrades the Colonic Mucus Barrier and Enhances Pathogen Susceptibility. Cell (2016) 167:1339–1353.e21. doi:10.1016/j.cell.2016.10.043 [PubMed: 27863247]
10. Hansen TH, Gøbel RJ, Hansen T, Pedersen O. The gut microbiome in cardio-metabolic health. Genome Med (2015) 7: doi:10.1186/s13073-015-0157-z
11. López P, De Paz B, Rodríguez-Carrio J, Hevia A, Sánchez B, Margolles A, Suárez A. Th17 responses and natural IgM antibodies are related to gut microbiota composition in systemic lupus erythematosus patients. Sci Rep (2016) 6:1–12. doi:10.1038/srep24072 [PubMed: 28442746]
12. Sanchez-Alcoholado L, Castellano-Castillo D, Jordán-Martínez L, Moreno-Indias I, Cardila-Cruz P, Elena D, Muñoz-Garcia AJ, Queipo-Ortuño MI, Jimenez-Navarro M. Role of gut microbiota on cardio-metabolic parameters and immunity in coronary artery disease patients with and without

type-2 diabetes mellitus. Front Microbiol (2017) 8:1–12. doi:10.3389/fmicb.2017.01936 [PubMed: 28197127]

13. Cryan JF, O'Mahony SM. The microbiome-gut-brain axis: From bowel to behavior. Neurogastroenterol Motil (2011) 23:187–192. doi:10.1111/j.1365-2982.2010.01664.x [PubMed: 21303428]
14. Rhee SH, Pothoulakis C, Mayer EA. Principles and clinical implications of the brain-gut-enteric microbiota axis. Nat Rev Gastroenterol Hepatol (2009) 6:306–314. doi:10.1038/nrgastro.2009.35 [PubMed: 19404271]
15. Lyte M. Microbial Endocrinology in the Microbiome-Gut-Brain Axis: How Bacterial Production and Utilization of Neurochemicals Influence Behavior. PLoS Pathog (2013) 9:9–11. doi:10.1371/journal.ppat.1003726
16. O'Toole PW, Jeffery IB. Microbiome–health interactions in older people. Cell Mol Life Sci (2018) 75:119–128. doi:10.1007/s00018-017-2673-z [PubMed: 28986601]
17. Nagpal R, Mainali R, Ahmadi S, Wang S, Singh R, Kavanagh K, Kitzman DW, Kushugulova A, Marotta F, Yadav H. Gut microbiome and aging: Physiological and mechanistic insights. Nutr Heal Aging (2018) 4:267–285. doi:10.3233/NHA-170030
18. Shibagaki N, Suda W, Clavaud C, Bastien P, Takayasu L, Iioka E, Kurokawa R, Yamashita N, Hattori Y, Shindo C, et al. Aging-related changes in the diversity of women's skin microbiomes associated with oral bacteria. Sci Rep (2017) 7:3–4. doi:10.1038/s41598-017-10834-9 [PubMed: 28127052]
19. Langille MGI, Meehan CJ, Koenig JE, Dhanani AS, Rose RA, Howlett SE, Beiko RG. Microbial shifts in the aging mouse gut. Microbiome (2014) 2: Available at: http://www.microbiomejournal.com/content/2/1/50
20. Bodogai M, O'Connell J, Kim K, Kim Y, Moritoh K, Chen C, Gusev F, Vaughan K, Shulzhenko N, Mattison JA, et al. Commensal bacteria contribute to insulin resistance in aging by activating innate B1a cells. Sci Transl Med (2018) 10:1–14. doi:10.1126/scitranslmed.aat4271
21. DeJong EN, Surette MG, Bowdish DME. The Gut Microbiota and Unhealthy Aging: Disentangling Cause from Consequence. Cell Host Microbe (2020) 28:180–189. doi:10.1016/j.chom.2020.07.013 [PubMed: 32791111]
22. Bana B, Cabreiro F. The Microbiome and Aging. Annu Rev Genet (2019) 53:239–261. doi:10.1146/annurev-genet-112618-043650 [PubMed: 31487470]
23. Bosco N, Noti M. The aging gut microbiome and its impact on host immunity. Genes Immun (2021) 22:289–303. doi:10.1038/s41435-021-00126-8 [PubMed: 33875817]
24. Kelly D, Mulder IE. Microbiome and immunological interactions. Nutr Rev (2012) 70: doi:10.1111/j.1753-4887.2012.00498.x
25. Levy M, Blacher E, Elinav E. Microbiome, metabolites and host immunity. Curr Opin Microbiol (2017) 35:8–15. doi:10.1016/J.MIB.2016.10.003 [PubMed: 27883933]
26. Thaiss CA, Zmora N, Levy M, Elinav E. The microbiome and innate immunity. Nature (2016) 535:65–74. doi:10.1038/nature18847 [PubMed: 27383981]
27. Mcdermott AJ, Huffnagle GB. The microbiome and regulation of mucosal immunity. Immunology (2014) 142:24–31. doi:10.1111/imm.12231 [PubMed: 24329495]
28. Hagan T, Cortese M, Rouphael N, Boudreau C, Linde C, Maddur MS, Das J, Wang H, Guthmiller J, Zheng NY, et al. Antibiotics-Driven Gut Microbiome Perturbation Alters Immunity to Vaccines in Humans. Cell (2019) 178:1313–1328.e13. doi:10.1016/j.cell.2019.08.010 [PubMed: 31491384]
29. Neish AS. Mucosal immunity and the microbiome. Ann Am Thorac Soc (2014) 11: doi:10.1513/AnnalsATS.201306-161MG
30. Baumgarth N. The Shaping of a B Cell Pool Maximally Responsive to Infections. Annu Rev Immunol (2021) 39:103–129. doi:10.1146/annurev-immunol-042718-041238 [PubMed: 33472004]
31. Belkaid Y, Hand TW. Role of the microbiota in immunity and inflammation. Cell (2014) 157:121–141. doi:10.1016/j.cell.2014.03.011 [PubMed: 24679531]
32. Brown EM, Sadarangani M, Finlay BB. The role of the immune system in governing host-microbe interactions in the intestine. Nat Immunol (2013) 14:660–667. doi:10.1038/ni.2611 [PubMed: 23778793]

33. Round JL, Mazmanian SK. The gut microbiota shapes intestinal immune responses during health and disease. Nat Rev Immunol (2009) 9:313–323. doi:10.1038/nri2515 [PubMed: 19343057]
34. Dominguez-Bello MG, Godoy-Vitorino F, Knight R, Blaser MJ. Role of the microbiome in human development. Gut (2019) 68:1108–1114. doi:10.1136/gutjnl-2018-317503 [PubMed: 30670574]
35. Petta I, Fraussen J, Somers V, Kleinewietfeld M. Interrelation of diet, gut microbiome, and autoantibody production. Front Immunol (2018) 9: doi:10.3389/fimmu.2018.00439
36. Silverman GJ. The microbiome in SLE pathogenesis. Nat Rev Rheumatol (2019) 15:72–74. doi:10.1038/s41584-018-0152-z [PubMed: 30607012]
37. Choi S-C, Brown J, Gong M, Ge Y, Zadeh M, Li W, Croker BP, Michailidis G, Garrett TJ, Mohamadzadeh M, et al. Gut microbiota dysbiosis and altered tryptophan catabolism contribute to autoimmunity in lupus-susceptible mice. Sci Transl Med (2020) 12: doi:10.1126/scitranslmed.aax2220
38. Potula H-HSK, Xu Z, Zeumer L, Sang A, Croker BP, Morel L. Cyclin-Dependent Kinase Inhibitor Cdkn2c Deficiency Promotes B1a Cell Expansion and Autoimmunity in a Mouse Model of Lupus. J Immunol (2012) 189:2931–2940. doi:10.4049/jimmunol.1200556 [PubMed: 22896639]
39. Blandino R, Baumgarth N. Secreted IgM: New tricks for an old molecule. J Leukoc Biol (2019) 106:1021–1034. doi:10.1002/JLB.3RI0519-161R [PubMed: 31302940]
40. Förster I, Rajewsky K. Expansion and functional activity of Ly-1+ B cells upon transfer of peritoneal cells into allotype-congenic, newborn mice. Eur J Immunol (1987) 17:521–528. doi:10.1002/EJI.1830170414 [PubMed: 2436924]
41. Lalor PA, Herzenberg LA, Adams S, Stall AM. Feedback regulation of murine Ly-1 B cell development. Eur J Immunol (1989) 19:507–513. doi:10.1002/EJI.1830190315 [PubMed: 2785046]
42. Ehrenstein MR, Notley CA. The importance of natural IgM: scavenger, protector and regulator. Nat Rev Immunol (2010) 10:778–786. doi:10.1038/NRI2849 [PubMed: 20948548]
43. Boes M, Esau C, Fischer MB, Schmidt T, Carroll M, Chen J. Enhanced B-1 cell development, but impaired IgG antibody responses in mice deficient in secreted IgM. J Immunol (1998) 160:4776–87. Available at: http://www.ncbi.nlm.nih.gov/pubmed/9590224 [PubMed: 9590224]
44. Nguyen TTT, Elsner RA, Baumgarth N. Natural IgM Prevents Autoimmunity by Enforcing B Cell Central Tolerance Induction. J Immunol (2015) 194:1489–1502. doi:10.4049/jimmunol.1401880 [PubMed: 25595791]
45. Tsiantoulas D, Kiss M, Bartolini-Gritti B, Bergthaler A, Mallat Z, Jumaa H, Binder CJ. Secreted IgM deficiency leads to increased BCR signaling that results in abnormal splenic B cell development. Sci Rep (2017) 7:1–9. doi:10.1038/s41598-017-03688-8 [PubMed: 28127051]
46. Ehrenstein MR, Cook HT, Neuberger MS. Deficiency in serum immunoglobulin (Ig)M predisposes to development of IgG autoantibodies. J Exp Med (2000) 191:1253–1257. doi:10.1084/jem.191.7.1253 [PubMed: 10748243]
47. Weksler ME, Pawelec G, Franceschi C. Immune therapy for age-related diseases. Trends Immunol (2009) 30:344–350. doi:10.1016/J.IT.2009.03.011 [PubMed: 19541533]
48. Binder CJ, Silverman GJ. Natural antibodies and the autoimmunity of atherosclerosis. Springer Semin Immunopathol (2005) 26:385–404. doi:10.1007/s00281-004-0185-z [PubMed: 15609021]
49. Kearney JF, Patel P, Stefanov EK, King RG. Natural Antibody Repertoires: Development and Functional Role in Inhibiting Allergic Airway Disease. Annu Rev Immunol (2015) 33:475–504. doi:10.1146/ANNUREV-IMMUNOL-032713-120140 [PubMed: 25622195]
50. Haas KM, Poe JC, Steeber DA, Tedder TF. B-1a and B-1b cells exhibit distinct developmental requirements and have unique functional roles in innate and adaptive immunity to S. pneumoniae. Immunity (2005) 23:7–18. doi:10.1016/j.immuni.2005.04.011 [PubMed: 16039575]
51. Webster SE, Ryali B, Clemente MJ, Tsuji N, Holodick NE. Sex Influences Age-Related Changes in Natural Antibodies and CD5+ B-1 Cells. J Immunol (2022) 208:1–17. [PubMed: 34933943]
52. Kaur H, Nookala S, Singh S, Mukundan S, Nagamoto-Combs K, Combs CK. Sex-Dependent Effects of Intestinal Microbiome Manipulation in a Mouse Model of Alzheimer's Disease. Cells (2021) 10:2370. doi:10.3390/CELLS10092370 [PubMed: 34572019]
53. Jašarević E, Morrison KE, Bale TL. Sex differences in the gut microbiome - Brain axis across the lifespan. Philos Trans R Soc B Biol Sci (2016) 371:12–17. doi:10.1098/rstb.2015.0122

54. Kaliannan K, Robertson RC, Murphy K, Stanton C, Kang C, Wang B, Hao L, Bhan AK, Kang JX. Estrogen-mediated gut microbiome alterations influence sexual dimorphism in metabolic syndrome in mice. Microbiome (2018) 6:1–22. doi:10.1186/s40168-018-0587-0 [PubMed: 29291746]
55. Markle JGM, Frank DN, Mortin-Toth S, Robertson CE, Feazel LM, Rolle-Kampczyk U, Von Bergen M, McCoy KD, MacPherson AJ, Danska JS. Sex Differences in the Gut Microbiome Drive Hormone-Dependent Regulation of Autoimmunity. Science (80-) (2013) 339:1084–1088.
56. Jašarević E, Hill EM, Kane PJ, Rutt L, Gyles T, Folts L, Rock KD, Howard CD, Morrison KE, Ravel J, et al. The composition of human vaginal microbiota transferred at birth affects offspring health in a mouse model. Nat Commun 2021 121 (2021) 12:1–16. doi:10.1038/s41467-021-26634-9
57. Fischinger S, Boudreau CM, Butler AL, Streeck H, Alter G. Sex differences in vaccine-induced humoral immunity. Semin Immunopathol (2019) 41:239–249. doi:10.1007/s00281-018-0726-5 [PubMed: 30547182]
58. Koelman L, Pivovarova-Ramich O, Pfeiffer AFH, Grune T, Aleksandrova K. Cytokines for evaluation of chronic inflammatory status in ageing research: Reliability and phenotypic characterisation. Immun Ageing (2019) 16:1–12. doi:10.1186/s12979-019-0151-1 [PubMed: 30679937]
59. Burrello C, Garavaglia F, Cribiù FM, Ercoli G, Lopez G, Troisi J, Colucci A, Guglietta S, Carloni S, Guglielmetti S, et al. Therapeutic faecal microbiota transplantation controls intestinal inflammation through IL10 secretion by immune cells. Nat Commun (2018) 9: doi:10.1038/s41467-018-07359-8
60. He B, Liu Y, Hoang TK, Tian X, Taylor CM, Luo M, Tran DQ, Tatevian N, Rhoads JM. Antibiotic-modulated microbiome suppresses lethal inflammation and prolongs lifespan in Treg-deficient mice. Microbiome (2019) 7:1–12. doi:10.1186/s40168-019-0751-1 [PubMed: 30606251]
61. Luckett-Chastain LR, King CJ, McShan WM, Gipson JR, Gillaspy AF, Gallucci RM. Loss of Interleukin-6 Influences Transcriptional Immune Signatures and Alters Bacterial Colonization in the Skin. Front Microbiol (2021) 12: doi:10.3389/fmicb.2021.658980
62. O'garra A, Chang R, Go N, Hastings R, Haughton G, Howard M. Ly-1 B (B-1) cells are the main source of B cell-derived interleukin 10. Eur J Immunol (1992) 22:711–717. doi:10.1002/eji.1830220314 [PubMed: 1547817]
63. O'garra A, Howard M. Cytokines and Ly-1 (B1) B Cells. Int Rev Immunol (1992) 8:219–234. doi:10.3109/08830189209055575 [PubMed: 1602214]
64. Kroese F, Bos N. Peritoneal B-1 cells switch in vivo to IgA and these IgA antibodies can bind to bacteria of the normal intestinal microflora. Curr Top Microbiol Immunol (1999) 246:343–350. Available at: https://research.rug.nl/en/publications/peritoneal-b-1-cells-switch-in-vivo-to-iga-and-these-iga-antibodi [Accessed March 2, 2022] [PubMed: 10396074]
65. Macpherson AJ, Gatto D, Sainsbury E, Harriman GR, Hengartner H, Zinkernagel R. A Primitive T Cell-Independent Mechanism of Intestinal Mucosal IgA Responses to Commensal Bacteria. Science (80-) (2000) 288:2222–2226. doi:10.1126/science.288.5474.2222
66. Kroese FGM, Butcher EC, Stall AM, Lalor PA, Adams S, Herzenberg LA. Many of the IgA producing plasma cells in murine gut are derived from self-replenishing precursors in the peritoneal cavity a. Int Immunol (1989) 1:75–84. doi:10.1093/intimm/1.1.75 [PubMed: 2487677]
67. Moon B, Takaki S, Miyake K, Takatsu K. The Role of IL-5 for Mature B-1 Cells in Homeostatic Proliferation, Cell Survival, and Ig Production. J Immunol (2004) 172:6020–6029. doi:10.4049/jimmunol.172.10.6020 [PubMed: 15128785]
68. Edgar RC. Search and clustering orders of magnitude faster than BLAST. Bioinformatics (2010) 26:2460–2461. doi:10.1093/bioinformatics/btq461 [PubMed: 20709691]
69. Edgar RC. UPARSE: highly accurate OTU sequences from microbial amplicon reads. Nat Methods (2013) 10:996–998. doi:10.1038/nmeth.2604 [PubMed: 23955772]
70. McDonald D, Price MN, Goodrich J, Nawrocki EP, DeSantis TZ, Probst A, Andersen GL, Knight R, Hugenholtz P. An improved Greengenes taxonomy with explicit ranks for ecological and evolutionary analyses of bacteria and archaea. ISME J (2012) 6:610–618. doi:10.1038/ismej.2011.139 [PubMed: 22134646]

71. Love MI, Huber W, Anders S. Moderated estimation of fold change and dispersion for RNA-seq data with DESeq2. Genome Biol (2014) 15:550. doi:10.1186/s13059-014-0550-8 [PubMed: 25516281]
72. Marín-Aguilar F, Ruiz-Cabello J, Cordero MD. “Aging and the Inflammasomes,” in Inflammasomes: Clinical and Therapeutic Implications, eds. Cordero MD, Alcocer-Gómez E (Cham: Springer International Publishing), 303–320. doi:10.1007/978-3-319-89390-7_13
73. Schirmer M, Smeekens SP, Vlamakis H, Jaeger M, Oosting M, Franzosa EA, Jansen T, Jacobs L, Bonder MJ, Kurilshikov A, et al. Linking the Human Gut Microbiome to Inflammatory Cytokine Production Capacity. Cell (2016) 167:1125–1136.e8. doi:10.1016/j.cell.2016.10.020 [PubMed: 27814509]
74. Franceschi C, Bonafè M, Valensin S, Olivieri F, De Luca M, Ottaviani E, De Benedictis G. Inflamm-aging. An evolutionary perspective on immunosenescence. Ann N Y Acad Sci (2000) 908:244–254. doi:10.1111/j.1749-6632.2000.tb06651.x [PubMed: 10911963]
75. Dabitao D, Margolick JB, Lopez J, Bream JH. Multiplex measurement of proinflammatory cytokines in human serum: Comparison of the Meso Scale Discovery electrochemiluminescence assay and the Cytometric Bead Array. J Immunol Methods (2011) 372:71–77. doi:10.1016/j.jim.2011.06.033 [PubMed: 21781970]
76. Feng E, Balint E, Poznanski SM, Ashkar AA, Loeb M. Aging and interferons: Impacts on inflammation and viral disease outcomes. Cells (2021) 10: doi:10.3390/cells10030708
77. Son DS, Parl AK, Rice VM, Khabele D. Keratinocyte chemoattractant (KC)/human growth-regulated oncogene (GRO) chemokines and pro-inflammatory chemokine networks in mouse and human ovarian epithelial cancer cells. Cancer Biol Ther (2007) 6:1308–1318. doi:10.4161/cbt.6.8.4506
78. Morley JE, Baumgartner RN. Cytokine-Related Aging Process. (2004) 59:924–929.
79. Banks WA, Farr SA, La Scola ME, Morley JE. Intravenous human interleukin-1 α impairs memory processing in mice: Dependence on blood-brain barrier transport into posterior division of the septum. J Pharmacol Exp Ther (2001) 299:536–541. [PubMed: 11602664]
80. Couper KN, Blount DG, Riley EM. IL-10: The Master Regulator of Immunity to Infection. J Immunol (2008) 180:5771–5777. doi:10.4049/jimmunol.180.9.5771 [PubMed: 18424693]
81. Dagdeviren S, Jung DY, Friedline RH, Noh HL, Kim JH, Patel PR, Tsitsilianos N, Inashima K, Tran DA, Hu X, et al. IL-10 prevents aging-associated inflammation and insulin resistance in skeletal muscle. FASEB J (2017) 31:701–710. doi:10.1096/fj.201600832R [PubMed: 27811060]
82. Lustig A, Liu HB, Metter EJ, An Y, Swaby MA, Elango P, Ferrucci L, Hodes RJ, Weng NP. Telomere shortening, inflammatory cytokines, and anti-cytomegalovirus antibody Follow Distinct ageassociated trajectories in humans. Front Immunol (2017) 8:4–11. doi:10.3389/fimmu.2017.01027 [PubMed: 28191005]
83. Lycke NY, Bemark M. The regulation of gut mucosal IgA B-cell responses: Recent developments. Mucosal Immunol (2017) 10:1361–1374. doi:10.1038/mi.2017.62 [PubMed: 28745325]
84. Duan B, Morel L. Role of B-1a cells in autoimmunity. Autoimmun Rev (2006) 5:403–408. doi:10.1016/j.autrev.2005.10.007 [PubMed: 16890894]
85. Tumang JR, Holodick NE, Vizconde TC, Kaku H, Francés R, Rothstein TL. A CD25- positive population of activated B1 cells expresses LIFR and responds to LIF. Front Immunol (2011) 2:1–8. doi:10.3389/fimmu.2011.00006 [PubMed: 22566792]
86. Jakobsson HE, Rodríguez-Piñeiro AM, Schütte A, Ermund A, Boysen P, Bemark M, Sommer F, Bäckhed F, Hansson GC, Johansson ME. The composition of the gut microbiota shapes the colon mucus barrier. EMBO Rep (2015) 16:164–177. doi:10.15252/embr.201439263 [PubMed: 25525071]
87. Kuehbacher T, Rehman A, Lepage P, Hellmig S, Fölsch UR, Schreiber S, Ott SJ. Intestinal TM7 bacterial phylogenies in active inflammatory bowel disease. J Med Microbiol (2008) 57:1569–1576. doi:10.1099/jmm.0.47719-0 [PubMed: 19018031]
88. Greer RL, Dong X, Moraes ACF, Zielke RA, Fernandes GR, Peremyslova E, Vasquez-Perez S, Schoenborn AA, Gomes EP, Pereira AC, et al. Akkermansia muciniphila mediates negative effects of IFNγ on glucose metabolism. Nat Commun (2016) 7:1–13. doi:10.1038/ncomms13329

89. Xu Y, Wang N, Tan HY, Li S, Zhang C, Feng Y. Function of Akkermansia muciniphila in Obesity: Interactions With Lipid Metabolism, Immune Response and Gut Systems. Front Microbiol (2020) 11:1–12. doi:10.3389/fmicb.2020.00219 [PubMed: 32082274]

90. Lecomte V, Kaakoush NO, Maloney CA, Raipuria M, Huinao KD, Mitchell HM, Morris MJ. Changes in gut microbiota in rats fed a high fat diet correlate with obesity-associated metabolic parameters. PLoS One (2015) 10: doi:10.1371/journal.pone.0126931

91. Wang Y, Ouyang M, Gao X, Wang S, Fu C, Zeng J, He X. Phocea, pseudoflavonifractor and Lactobacillus intestinalis: Three potential biomarkers of gut microbiota that affect progression and complications of obesity-induced type 2 diabetes mellitus. Diabetes, Metab Syndr Obes Targets Ther (2020) 13:835–850. doi:10.2147/DMSO.S240728

92. Kovacs A, Ben-Jacob N, Tayem H, Halperin E, Iraqi FA, Gophna U. Genotype Is a Stronger Determinant than Sex of the Mouse Gut Microbiota. Microb Ecol (2011) 61:423–428. doi:10.1007/s00248-010-9787-2 [PubMed: 21181142]

93. Rausch P, Basic M, Batra A, Bischoff SC, Blaut M, Clavel T, Gläsner J, Gopalakrishnan S, Grassl GA, Günther C, et al. Analysis of factors contributing to variation in the C57BL/6J fecal microbiota across German animal facilities. Int J Med Microbiol (2016) 306:343–355. doi:10.1016/j.ijmm.2016.03.004 [PubMed: 27053239]

94. Petkova SB, Yuan R, Tsaih SW, Schott W, Roopenian DC, Paigen B. Genetic influence on immune phenotype revealed strain-specific variations in peripheral blood lineages. Physiol Genomics (2008) 34:304–314. doi:10.1152/physiolgenomics.00185.2007 [PubMed: 18544662]

95. Ivanov II, Atarashi K, Manel N, Brodie EL, Shima T, Karaoz U, Wei D, Goldfarb KC, Santee CA, Lynch SV., et al. Induction of Intestinal Th17 Cells by Segmented Filamentous Bacteria. Cell (2009) 139:485–498. doi:10.1016/j.cell.2009.09.033 [PubMed: 19836068]

96. Zheng D, Liwinski T, Elinav E. Interaction between microbiota and immunity in health and disease. Cell Res (2020) 30:492–506. doi:10.1038/s41422-020-0332-7 [PubMed: 32433595]

97. Rea IM, Gibson DS, McGilligan V, McNerlan SE, Denis Alexander H, Ross OA. Age and age-related diseases: Role of inflammation triggers and cytokines. Front Immunol (2018) 9:1–28. doi:10.3389/fimmu.2018.00586 [PubMed: 29403488]

98. Liu Y, Chen H, Feng L, Zhang J. Interactions between gut microbiota and metabolites modulate cytokine network imbalances in women with unexplained miscarriage. npj Biofilms Microbiomes (2021) 7:24. doi:10.1038/s41522-021-00199-3 [PubMed: 33731680]

99. Guo Y, Wang B, Wang T, Gao L, Yang ZJ, Wang FF, Shang HW, Hua R, Xu JD. Biological characteristics of il-6 and related intestinal diseases. Int J Biol Sci (2020) 17:204–219. doi:10.7150/ijbs.51362

100. Marie, Brambilla IJ, Azzouz L, Chen D, Baracho Z, Arnett GV, Li A, Liu HS, Cimmino W, Chattopadhyay L, Silverman P, Watowich G, Khor SS, Levy DE B. Tonic interferon restricts pathogenic IL-17-driven inflammatory disease via balancing the microbiome. Elife (2021) 2021;10:e6: doi:10.7554/eLife.68371

101. Morhardt TL, Hayashi A, Ochi T, Quirós M, Kitamoto S, Nagao-Kitamoto H, Kuffa P, Atarashi K, Honda K, Kao JY, et al. IL-10 produced by macrophages regulates epithelial integrity in the small intestine. Sci Rep (2019) 9:1–10. doi:10.1038/s41598-018-38125-x [PubMed: 30626917]

102. Mishima Y, Oka A, Liu B, Herzog JW, Eun CS, Fan TJ, Bulik-Sullivan E, Carroll IM, Hansen JJ, Chen L, et al. Microbiota maintain colonic homeostasis by activating TLR2/MyD88/PI3K signaling in IL-10-producing regulatory B cells. J Clin Invest (2019) 129:3702–3716. doi:10.1172/JCI93820 [PubMed: 31211700]

103. Mohamad N-V, Wong SK, Wan Hasan WN, Jolly JJ, Nur-Farhana MF, Ima-Nirwana S, Chin K-Y. The relationship between circulating testosterone and inflammatory cytokines in men. Aging Male (2019) 22:129–140. doi:10.1080/13685538.2018.1482487 [PubMed: 29925283]

104. Daynes RA, Dudley DJ, Araneo BA. Regulation of murine lymphokine production in vivo II. Dehydroepiandrosterone is a natural enhancer of interleukin 2 synthesis by helper T cells. Eur J Immunol (1990) 20:793–802. doi:10.1002/eji.1830200413 [PubMed: 2140789]

105. Suzuki T, Suzuki N, Daynes RA, Engleman EG. Dehydroepiandrosterone enhances IL2 production and cytotoxic effector function of human T cells. Clin Immunol Immunopathol (1991) 61:202–211. doi:10.1016/S0090-1229(05)80024-8 [PubMed: 1833106]

106. Clarke G, Stilling RM, Kennedy PJ, Stanton C, Cryan JF, Dinan TG. Minireview: Gut Microbiota: The Neglected Endocrine Organ. Mol Endocrinol (2014) 28:1221–1238. [PubMed: 24892638]

107. Ruan W, Engevik MA, Spinler JK, Versalovic J. Healthy Human Gastrointestinal Microbiome: Composition and Function After a Decade of Exploration. Dig Dis Sci (2020) 65:695–705. doi:10.1007/s10620-020-06118-4 [PubMed: 32067143]

108. Tuck CJ, De Palma G, Takami K, Brant B, Caminero A, Reed DE, Muir JG, Gibson PR, Winterborn A, Verdu EF, et al. Nutritional profile of rodent diets impacts experimental reproducibility in microbiome preclinical research. Sci Rep (2020) 10:17784. doi:10.1038/s41598-020-74460-8 [PubMed: 33082369]

109. Ijaz MU, Ahmed MI, Zou X, Hussain M, Zhang M, Zhao F, Xu X, Zhou G, Li C. Beef, Casein, and Soy Proteins Differentially Affect Lipid Metabolism, Triglycerides Accumulation and Gut Microbiota of High-Fat Diet-Fed C57BL/6J Mice. Front Microbiol (2018) 9: Available at: https://www.frontiersin.org/articles/10.3389/fmicb.2018.02200

110. Margry B, Kersemakers SCW, Hoek A, Arkesteijn GJA, Wieland WH, Van Eden W, Broere F. Activated peritoneal cavity B-1a cells possess regulatory B cell properties. PLoS One (2014) 9: doi:10.1371/journal.pone.0088869

111. Cebra JJ, Bos NA, Cebra ER, Cuff CF, Deenen GJ, Kroese FG, Shroff KE. Development of components of the mucosal immune system in SCID recipient mice. Adv Exp Med Biol (1994) 355:255–259. doi:10.1007/978-1-4615-2492-2_43 [PubMed: 7709831]

112. Kroese FG, de Waard R, Bos NA. B-1 cells and their reactivity with the murine intestinal microflora. Semin Immunol (1996) 8:11–18. doi:10.1006/smim.1996.0003 [PubMed: 8850294]

113. Snider DP, Liang H, Switzer I, Underdown BJ. IgA production in MHC class II-deficient mice is primarily a function of B-1α cells. Int Immunol (1999) 11:191–198. doi:10.1093/intimm/11.2.191 [PubMed: 10069417]

114. Azzam KM, Madenspacher JH, Cain DW, Lai L, Gowdy KM, Rai P, Janardhan K, Clayton N, Cunningham W, Jensen H, et al. Irgm1 coordinately regulates autoimmunity and host defense at select mucosal surfaces. JCI insight (2017) 2:1–16. doi:10.1172/jci.insight.91914

115. Zhang H, Sparks JB, Karyala SV., Settlage R, Luo XM. Host adaptive immunity alters gut microbiota. ISME J (2015) 9:770–781. doi:10.1038/ismej.2014.165 [PubMed: 25216087]

116. King KY, Baldridge MT, Weksberg DC, Chambers SM, Lukov GL, Wu S, Boles NC, Jung SY, Qin J, Liu D, et al. Irgm1 protects hematopoietic stem cells by negative regulation of IFN signaling. Blood (2011) 118:1525–1533. [PubMed: 21633090]

117. Taylor GA, Huang H, Fee BE, Youssef N, Jewell ML, Cantillana V, Schoenborn AA, Rogala AR, Buckley AF, Feng CG, et al. Irgm1-deficiency leads to myeloid dysfunction in colon lamina propria and susceptibility to the intestinal pathogen Citrobacter rodentium. PLoS Pathog (2020) 16: doi:10.1371/journal.ppat.1008553

118. Liu B, Gulati AS, Cantillana V, Henry SC, Schmidt EA, Daniell X, Grossniklaus E, Schoenborn AA, Sartor RB, Taylor GA. Irgm1-deficient mice exhibit paneth cell abnormalities and increased susceptibility to acute intestinal inflammation. Am J Physiol - Gastrointest Liver Physiol (2013) 305:573–584. doi:10.1152/ajpgi.00071.2013

119. RA J, HA J, lan AR, Shisan B, MK I, Georges K, Manfred K. The Role of Interleukin-6 in Mucosal IgA Antibody Responses in Vivo. Science (80-) (1994) 264:561–563. doi:10.1126/science.8160012

120. Low A, Soh M, Miyake S, Seedorf H. Host Age Prediction from Fecal Microbiota Composition in Male C57BL/6J Mice. Microbiol Spectr (2022) 10:e00735–22. doi:10.1128/spectrum.00735-22 [PubMed: 35674443]

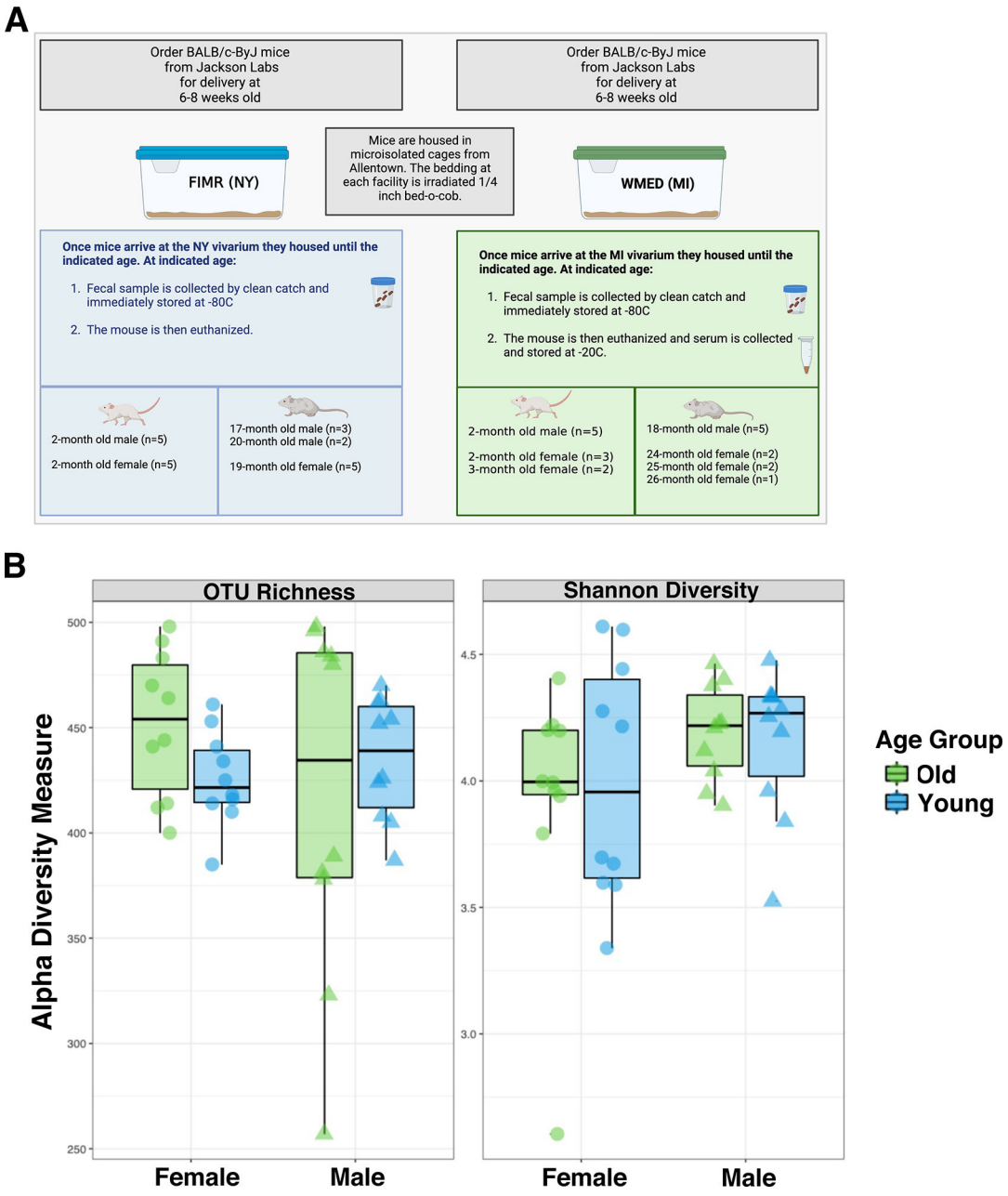

Figure 1. Experimental design and alpha diversity estimate between groups show no significant differences between males and females for whole microbiome analysis

(A) Experimental design. Samples from BALB/c-ByJ mice were collected at two different locations: The Feinstein Institute for Medical Research (FIMR) and Western Michigan University Homer Stryker M.D. School of Medicine (WMed). Mice were purchased from Jackson Laboratory at 6 weeks of age and then housed in the respective animal facility until the aged indicated. **(B)** Alpha diversity was analyzed by two means: OTU richness and the Shannon diversity index. OTU richness represents the number of OTUs present in each sample. Young mice are blue and old mice are green. The female mice had an OTU richness of 434±65.3 while the male mice had an OTU richness of 430±25.6 (p=0.3). The

Shannon diversity index considers the richness and evenness of OTUs within a sample and was calculated to be 3.97±0.475 for female mice and 4.17±0.24 for male mice (p=0.77). Statistics used = Kruskal-Wallis

A

Microbiome Covariate Significance with distance measurements via PERMANOVA

Variable	Classes	Sample Count (*n*)	*P*-value
Individual Age	2mo, 4mo, 17mo, 18mo, 19mo, 20mo, 24mo, 25mo, 26mo	18, 2, 3, 5, 5, 2, 2, 1, 2	0.001
Age Group	Old, Young	20, 20	0.001
Sex	Female, Male	20, 20	0.001
Location	Batch 1, Batch 2	20, 20	0.001
Young Sex	Young male vs young female	10, 10	0.003
Aged Sex	Old male vs old female	10, 10	0.003
Males	Old, Young	10, 10	0.001
Females	Old, Young	10, 10	0.001

B

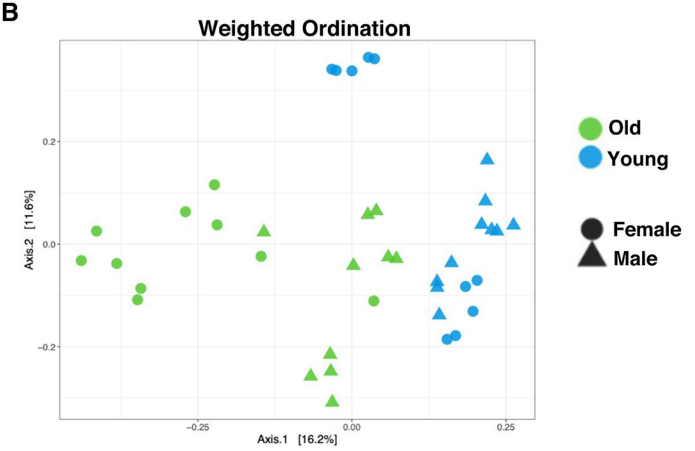

C

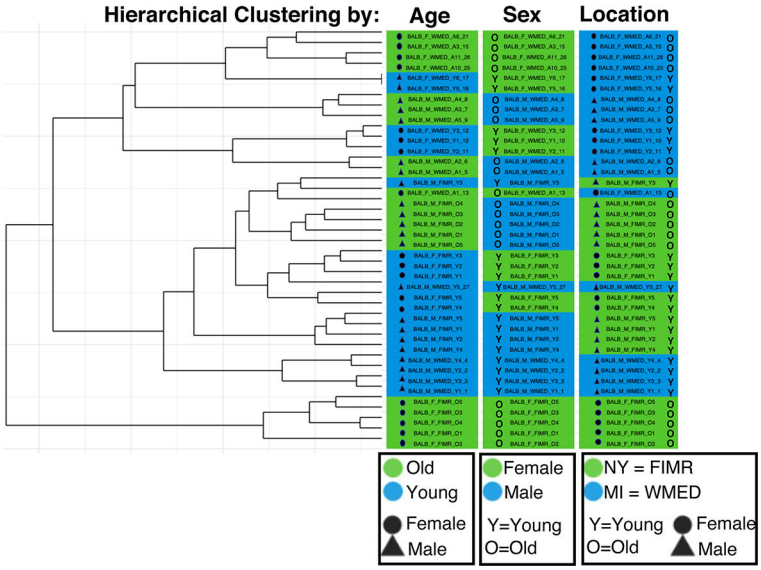

Figure 2. Beta diversity analysis shows significant contributions from age, sex, and location on microbiota

(A) Microbiome covariate significance was measured with distance measurements via PERMANOVA. Each variable tested is listed with relative classes, n for each class, and calculated p-value. **(B)** Weighted ordination by dimensional reduction of the Bray-Curtis dissimilarity between microbiome samples, using the PCoA ordination method shows that samples separated by age group (p=0.001) and sex (p=0.001). To further examine these relationships, samples were clustered by the Ward's method and Bray-Curtis distance. **(C)**

Hierarchical clustering partially separated by age, sex, and location. A PERMANOVA using distance matrices was performed for each variable of interest to determine if they significantly contributed to the beta diversity of the samples. All variables tested had a statistical significance of $p < 0.01$ when tested separately.

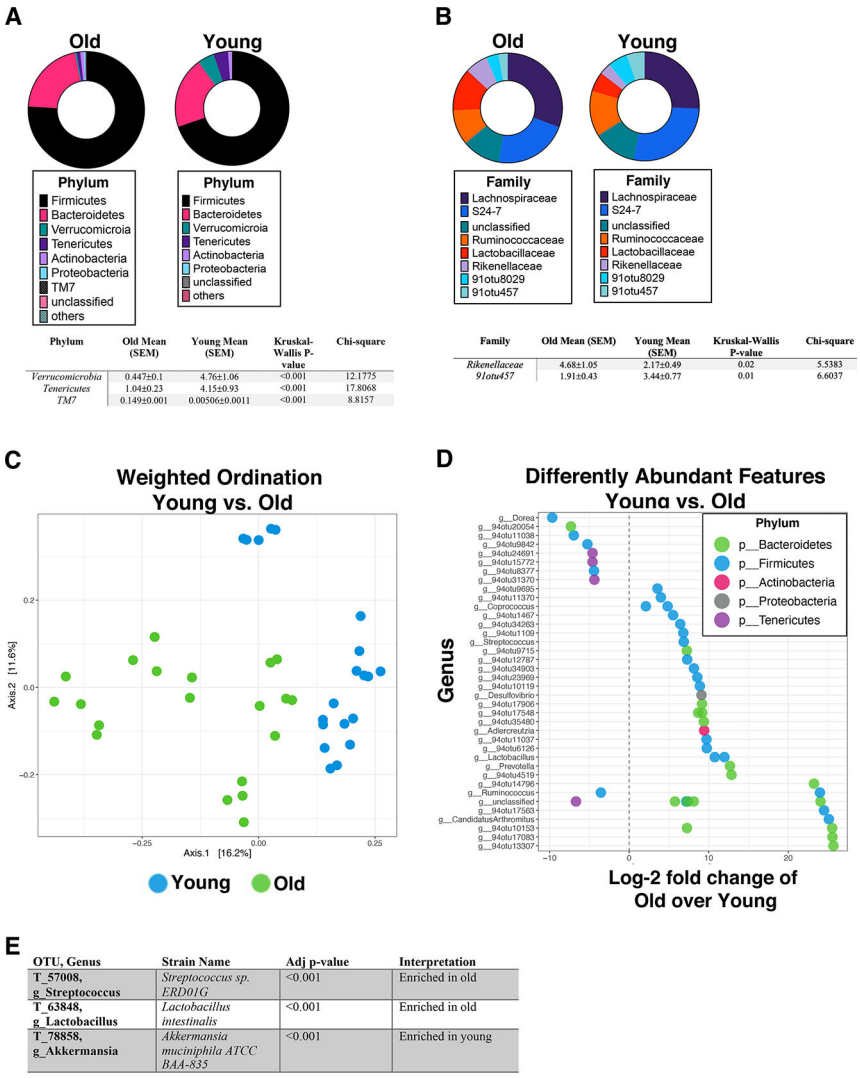

Phylum	Old Mean (SEM)	Young Mean (SEM)	Kruskal-Wallis P-value	Chi-square
Verrucomicrobia	0.447±0.1	4.76±1.06	<0.001	12.1775
Tenericutes	1.04±0.23	4.15±0.93	<0.001	17.8068
TM7	0.149±0.001	0.00506±0.0011	<0.001	8.8157

Family	Old Mean (SEM)	Young Mean (SEM)	Kruskal-Wallis P-value	Chi-square
Rikenellaceae	4.68±1.05	2.17±0.49	0.02	5.5383
91otu457	1.91±0.43	3.44±0.77	0.01	6.6037

E

OTU, Genus	Strain Name	Adj p-value	Interpretation
T_57008, g_Streptococcus	*Streptococcus sp. ERD01G*	<0.001	Enriched in old
T_63848, g_Lactobacillus	*Lactobacillus intestinalis*	<0.001	Enriched in old
T_78858, g_Akkermansia	*Akkermansia muciniphila ATCC BAA-835*	<0.001	Enriched in young

Figure 3. Age significantly impacts gut microbiome abundance and diversity

Percent abundance as means with SEM for the top eight phylum **(A)** and families **(B)** expressed between all aged mice vs all young mice. The two OTUs listed (91otu8029 and 91otu457) belong to the Clostridiales Family. Significant changes ($p<0.05$) are indicated the in the tables below each plot. **(C)** Weighted ordination by abundance indicates that samples cluster by age and partially by sex. **(D)** Top 50 significantly differently expressed OTUs between all aged mice vs young mice by phylum are represented out of a total of 170 significantly different features. **(E)** The feature selection summary for 6 OTUs identified at the strain level. Significance was tested using a negative binominal noise model with Poisson process corrected for FDR with Benjamini-Hochberg procedure.

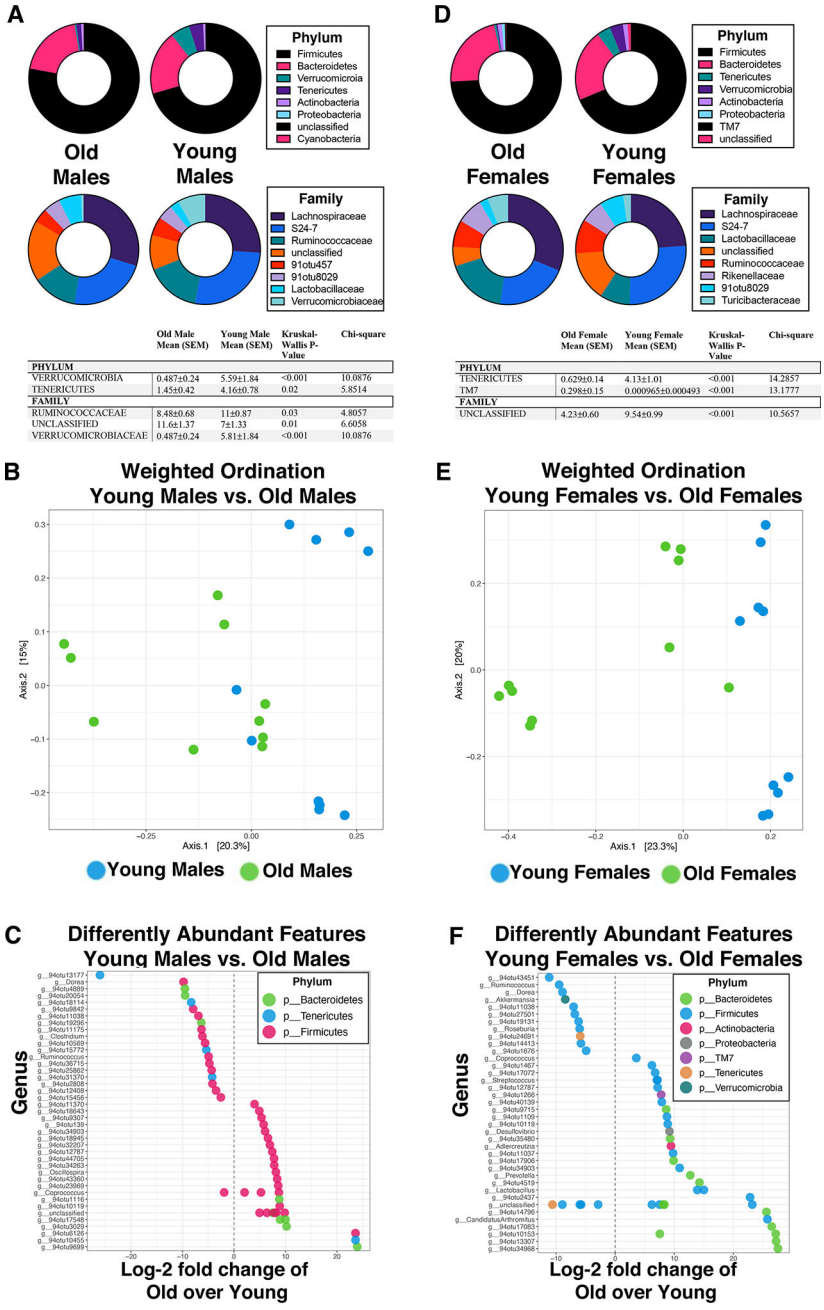

Figure 4. Aging in a sex-independent manner significantly changes the diversity and abundance of the gut microbiome in mice

(A, D) Percent abundance as means with SEM for the top eight phylum and families expressed between aged and young male **(A)** and female **(D)** mice. The two OTUs listed (91otu8029 and 91otu457) belong to the Clostridiales Family. Significant changes ($p<0.05$) are indicated the in the tables. **(B, E)** Weighted ordination by abundance indicates that samples cluster by age for males **(B)** and by age for females **(E)**. **(C, F)** Top 50 significantly differently expressed OTUs. Significance was tested using a negative binominal noise model with Poisson process corrected for FDR with Benjamini-Hochberg procedure.

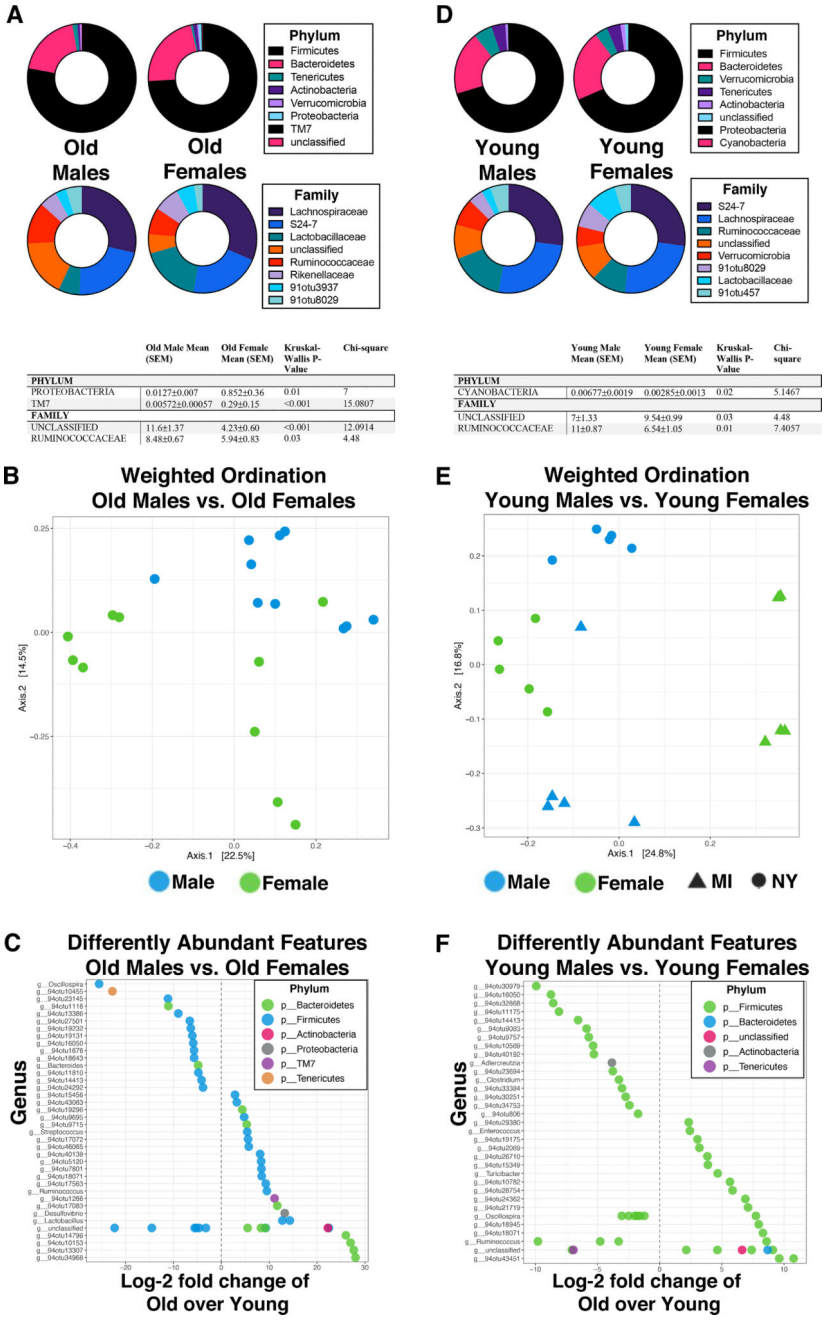

	Old Male Mean (SEM)	Old Female Mean (SEM)	Kruskal-Wallis P-Value	Chi-square
PHYLUM				
PROTEOBACTERIA	0.0127±0.007	0.852±0.36	0.01	7
TM7	0.00572±0.00057	0.29±0.15	<0.001	15.0807
FAMILY				
UNCLASSIFIED	11.6±1.37	4.23±0.60	<0.001	12.0914
RUMINOCOCCACEAE	8.48±0.67	5.94±0.83	0.03	4.48

	Young Male Mean (SEM)	Young Female Mean (SEM)	Kruskal-Wallis P-Value	Chi-square
PHYLUM				
CYANOBACTERIA	0.00677±0.0019	0.00285±0.0013	0.02	5.1467
FAMILY				
UNCLASSIFIED	7±1.33	9.54±0.99	0.03	4.48
RUMINOCOCCACEAE	11±0.87	6.54±1.05	0.01	7.4057

Figure 5. Biological sex directly influences the abundance and diversity of the gut microbiome in an age-independent mechanism in mice

(A, D) Percent abundance as means with SEM for the top eight phylum and families expressed between old males and old females **(A)** and young males and young females **(D).** The two OTUs listed (91otu8029 and 91otu457) belong to the Clostridiales Family. Significant changes ($p<0.05$) are indicated the in the tables below each plot. **(B, E)** Weighted ordination by abundance indicates that samples cluster by age and partially by sex for males **(B)**, and by sex and location for females **(E)**. **(C,F)** Top 50 significantly differently

expressed OTUs. Significance was tested using a negative binominal noise model with Poisson process corrected for FDR with Benjamini-Hochberg procedure.

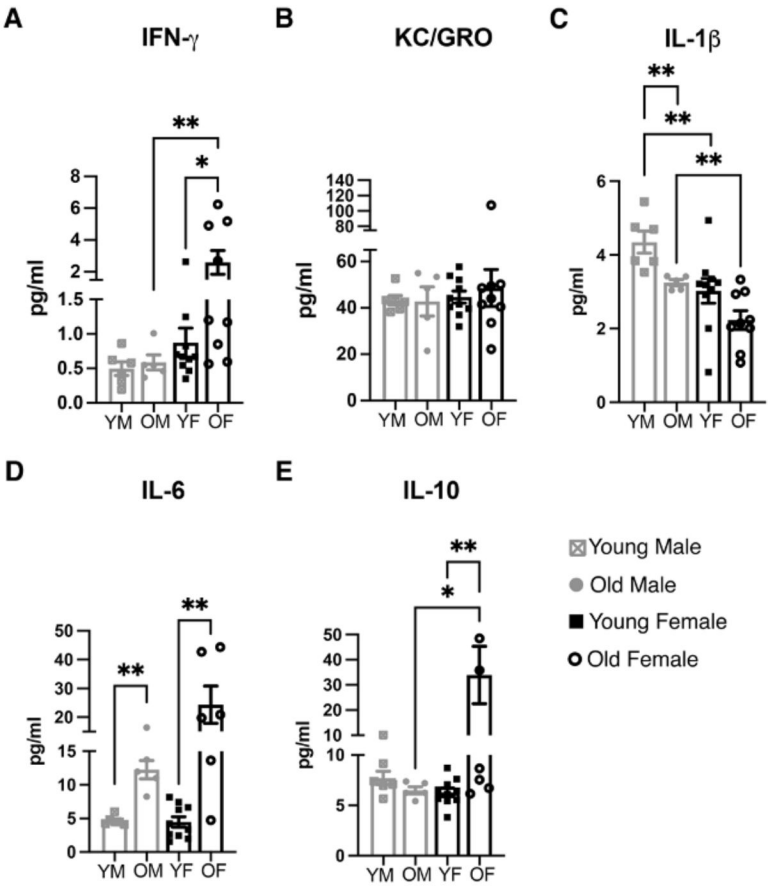

Figure 6. Cytokine biomarkers for inflammation and immune activation are influenced in a sex- and age-dependent mechanism

IFNy, IL-10, IL-1B, IL-5, IL-6, and KC/GRO were measured in serum obtained from BALB/c-ByJ mice located at WMed, this MI location. Concentrations (in pg/mL) were then averaged (error bars = SEM) for each sex and age group (n=5 old male, n=6 young male, n=9 old female, n=10 young female). Pair-wise comparisons were made using the Mann-Whitney test. Asterisks for p values: *p<0.05, **p<0.01.

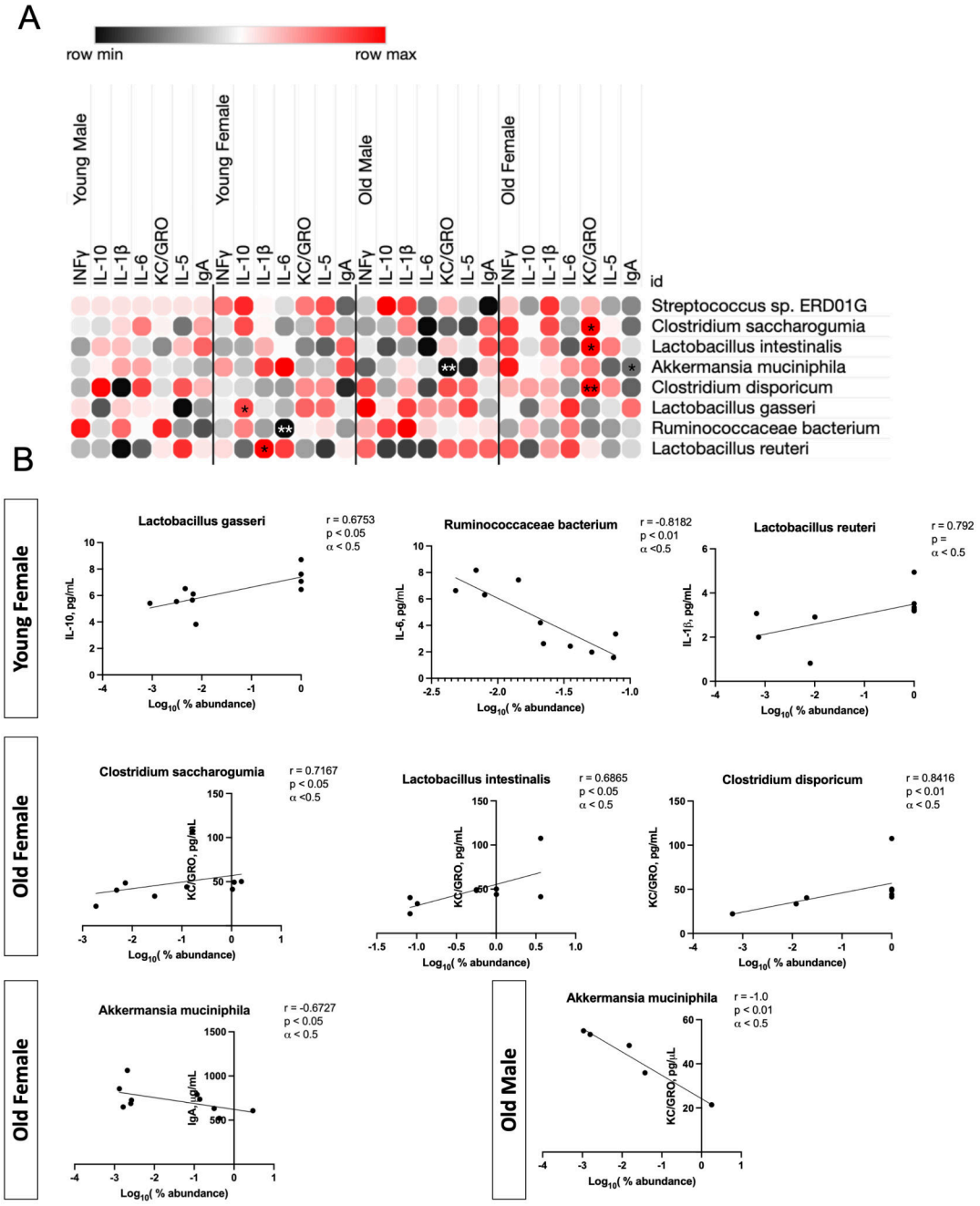

Figure 7. Significant correlations between gut microbial abundances and cytokine response are found in context to aging in a sex-dependent manner.

Summary of specific species associations with cytokine responses using Spearman correlation (α <0.05). All species were required to be present in >20% of all samples. Those with positive correlations are shown in red and those with negative correlations are shown in black. **(A)** shows the correlations for percent abundance of each strain and cytokine for each individual group (* p<0.05, ** p<0.01, *** p<0.001). **(B)** Each significant correlation was plotted, and the associated Spearman correlation value (r) was shown in reference to cytokine concentration (pg/mL) and the $\log_{10}$(% abundance) of each microbe.

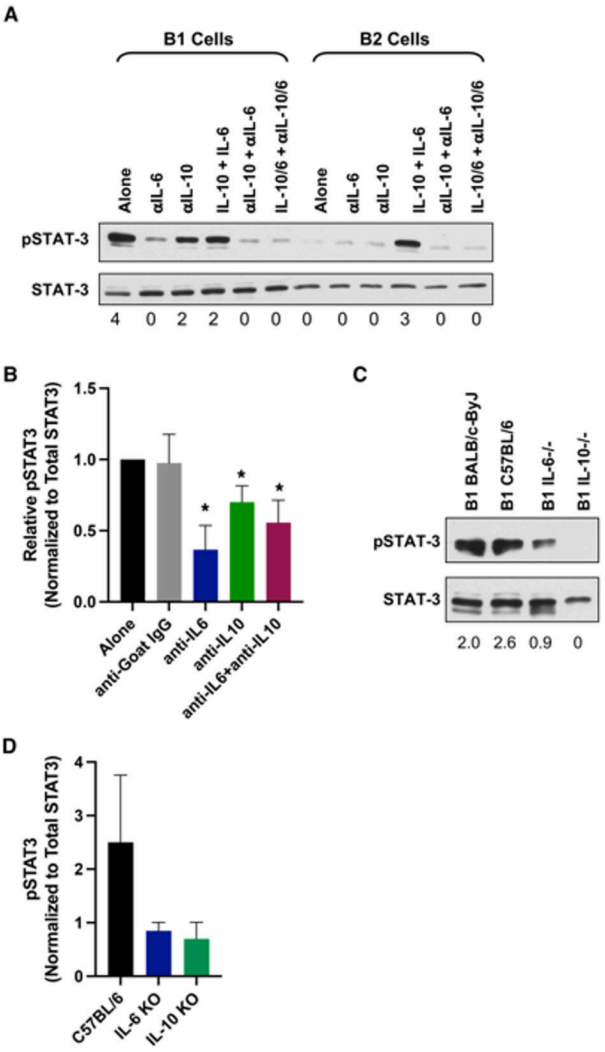

Figure 8. IL-6 and IL-10 provide the signal to constitutive pSTAT3 in CD5+ B-1 cells

(A) Sorted CD5+ B-1 and B-2 cells were treated for 24 hours as indicated with IL-10 (10 ng/ml), IL-6 (10 ng/ml), anti-IgG (10 μg/ml), anti-IL10 (10 μg/ml), and/or anti-IL-6 (10 μg/ml). Afterwards, cells were harvested to assess pSTAT3 levels by western blot analysis. Numbers below each band represent relative amount of phospho protein normalized to total STAT3. **(B)** Relative pSTAT3 protein expression normalized to total STAT3; average of four independent experiments. Significance was determined with the Mann-Whitney U test. **(C)** CD5+ B-1 cells were obtained from IL-6 or IL-10 knockout mice and assessed for pSTAT3 by western blot analysis. Numbers below each band represent relative amount of phospho protein normalized to total STAT3. **(D)** Relative pSTAT3 protein expression normalized to total STAT3; average of four independent experiments. Significance was determined with the Mann-Whitney U test.

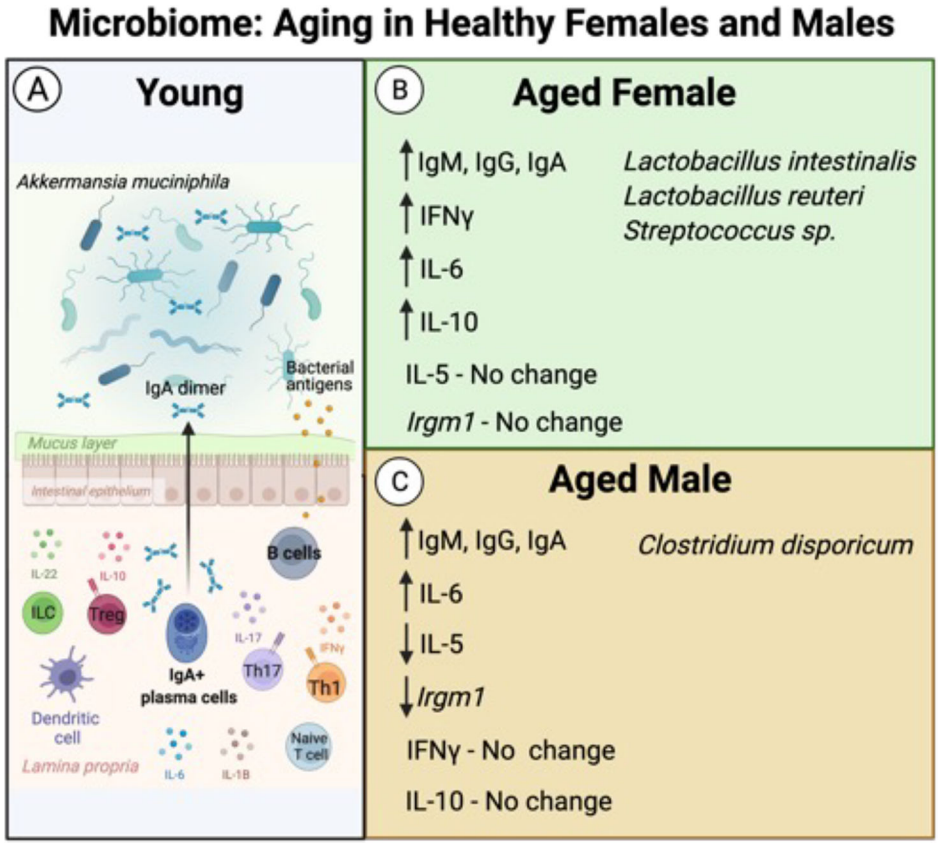

Figure 9. Summary of Microbiome and Immune System Aging in Healthy Females and Males.

The composition of the microbiome of young mice **(A)** is maintained by a complex interplay of both adaptive and innate immune cells and cytokines. IgA secreted by B lymphocytes is important for maintenance of beneficial bacteria, such as *A. muciniphila*. During the aging process, the microbiome is influenced in a sex-dependent manner. **(B)** Aged females have increased expression of IgM, IgG, and IgA, as well as increased serum levels of IFNγ, IL-6, and IL-10. There is no change in expression of IL-5 as compared to young animals. These changes are correlated with increased abundance of *L. intestinalis*, *L. reuteri*, and *Streptococcus* sp. **(C)** Aged males have increased production of IgM, IgG, and IgA as well as IL-6 but have decreased expression of IL-5. There are no changes in serum expression levels of IFNγ nor in IL-10. These changes in expression are correlated with increased abundance of *C. disporicum*. Figure was created with BioRender.com.